(NASA-CR-134282) SPACE SHUTTLE ORBIT MANEUVERING ENGINE REUSABLE THRUST CHAMBER: ADVERSE OPERATING CONDITIONS TEST REPORT (Rocketdyne) 66 p HC $6.25 CSCL 21H G3/28

N74-26247

Unclas
39783

Rocketdyne Division
Rockwell International

ASR74-131

SPACE SHUTTLE
ORBIT MANEUVERING ENGINE
REUSABLE THRUST CHAMBER

(NAS9-12802)

ADVERSE OPERATING CONDITIONS
TEST REPORT

ASR74-131

SPACE SHUTTLE
ORBIT MANEUVERING ENGINE
REUSABLE THRUST CHAMBER

(NAS9-12802)

ADVERSE OPERATING CONDITIONS
TEST REPORT

Prepared for

National Aeronautics and Space Administration
Johnson Spacecraft Center
Houston, Texas

Prepared by

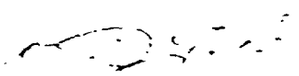

R. D. Tobin
Advanced Projects

Approved by

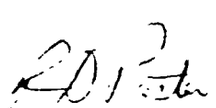

R. D. Paster
SS/OME Project Engineer
Advanced Programs

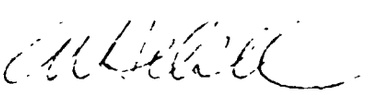

R. W. Helsel
SS/OME Program Manager
Advanced Programs

ROCKETDYNE DIVISION OF ROCKEWELL INTERNATIONAL CORPORATION
6633 CANOGA AVENUE, CANOGA PARK, CA 91304

FOREWORD

This report, prepared in accordance with G.O. 07634 is submitted in accordance with Contract NAS9-12802, Exhibit A (Statement of Work), Task IX (Adverse Operating Conditions).

ABSTRACT

Reported herein are descriptions of the test hardware, facility, procedures, and results of electrically heated tube and channel tests conducted to determine adverse operating condition limits for convectively cooled chambers typical of Space Shuttle Orbit Manuevering Engine designs. Hot-start tests were conducted with CRES and nickel tubes with both MMH and 50-50 coolants. Helium ingestion, in both bubble and froth form, was studied in tubular test sections. Helium bubble ingestion and burn-out limits in rectangular channels were also investigated.

INTRODUCTION

Under Task VII of the SS/OME Reusable Thrust Chamber Contract (NAS9-12802), heated tube tests were conducted with MMH and 50-50 fuels to establish convective cooling safety factor correlations for steady-state conditions. These correlations were used to design two regeneratively cooled thrust chambers which were subsequently satisfactorily operated over a wide range of chamber pressures and mixture ratios simulating OME operating conditions Adverse operating conditions have been identified which could be more severe than those previously tested. Rather than subject a complete regeneratively cooled thrust chamber to these conditions, an electrically heated tube test program was conducted (Task IX) in order to economically provide preliminary data to assess the impact of the adverse conditions on chamber operation.

The latest Space Shuttle flight plan requires that the OME start during the ascent trajectory. Thermal analyses have indicated that the inlet manifold and adjacent nozzle region may be several hundred degrees F due to heating from the SSME and SRB engines when the OME starts. Tests were, therefore, conducted in this task to demonstrate the maximum wall temperature at which the OME can safely start.

Although OMS pod specifications require that propellants be delivered to the OME free from helium bubbles or froth, the possibility exists that failure of a surface tension device could result in either form of helium being delivered to the engine. Tests were conducted in this task to determine the cooling correlations with frothed fuel and the maximum size helium bubbles which the regeneratively cooled chamber can tolerate.

Regenerative cooling safety factors are defined as the heat flux which results in transition to film boiling divided by the predicted heat

flux at the particular location in the chamber. The transition heat flux has been determined experimentally with one-dimensional heat flow through circular tubes (Task VII). The predicted heat flux is calculated using two-dimensional analysis. In the throat region, two-dimensional effects are negligible. At the injector end, however, the heat fluxes at the intersection of the land and hot wall are significantly higher than average. Safety factors are calculated based on these high heat fluxes. It has been shown, analytically, that local film boiling in the corners may be possible without burnout. Two-dimensional tests using asymmetrically heated rectangular passage test sections were conducted to determine burnout heat flux values for the injector end of the OME thrust chamber. Helium ingestion tests were also conducted with the 2-D test sections.

Testing was conducted at the Thermal Laboratory of the L.A. Division of Rockwell International, where the previous heated tube tests were run. The initial test program was performed in July 1973. Additional testing was accomplished in November-December 1973.

SUMMARY

A total of 44 hot-start simulation tests were conducted with MMH and 50-50 fuel coolants in both CRES and nickel tubes. Maximum test section temperatures as high as 1600 F were rapidly quenched without incident at coolant velocities as low as 5 ft/sec.

Eighty-two helium bubble tests were conducted with MMH and 50-50 fuel coolants in both CRES tubes and CRES asymmetrically heated rectangular passage test sections. Helium bubble durations in excess of one second were successfully achieved in the rectangular 2-D test section at the nominal OME thrcat heat flux level of 2.8 BTU/in^2-sec.

A total of 18 helium froth tests were conducted with MMH and 50-50 fuel coolants in CRES tubes. Helium froth flowrates as high as 30 percent (by volume) were achieved without significant wall temperature increases at the nominal injector end heat flux level of 1.5 BTU/in^2-sec. Five of the tests determined burn-out limits with various froth volume percents at increased heat flux levels.

Seven burn-out tests were conducted in the 2-D rectangular passage test sections. A maximum heat flux level of 4.1 BTU/in^2-sec was achieved at a value of $\dot{V} \cdot \Delta T_{SUB} = 9500 \frac{ft\text{-}F}{sec}$. This 2-D heat flux level is about one-half of that achieved in a circular tube at a similar $\dot{V} \cdot \Delta T_{SUB}$ value. At lower values of $\dot{V} \cdot \Delta T_{SUB} (< 3000 \frac{ft\text{-}F}{sec})$ the 2-D and 1-D burn-out heat flux levels are similar.

DISCUSSION

TEST FACILITY AND INSTRUMENTATION

Tests were conducted at the Los Angeles Division Thermal Laboratory, where previous OME heated tube test programs were conducted. The facility is shown schematically in Fig. 1. Coolant flows from the pressurized tank through shutoff, throttle, and check valves into the test section. Flowrate is measured by turbine flowmeter and calibrated orifice. A glass viewing section is installed downstream of the test section for visual and photographic observation of the flow with helium ingestion.

The test section consists of an electrically heated tube or channel section in a GN_2-purged box for safety (Fig. 2). Inlet and outlet pressures and temperatures of the coolant are measured. Wall temperatures are measured to indicate the onset of film boiling. Heating rates are controlled by the voltage applied to the ends of the test section via terminal bars. A back pressure regulator maintains the desired pressure at the end of the test section. GN_2 is used to purge the test section container and the flow system.

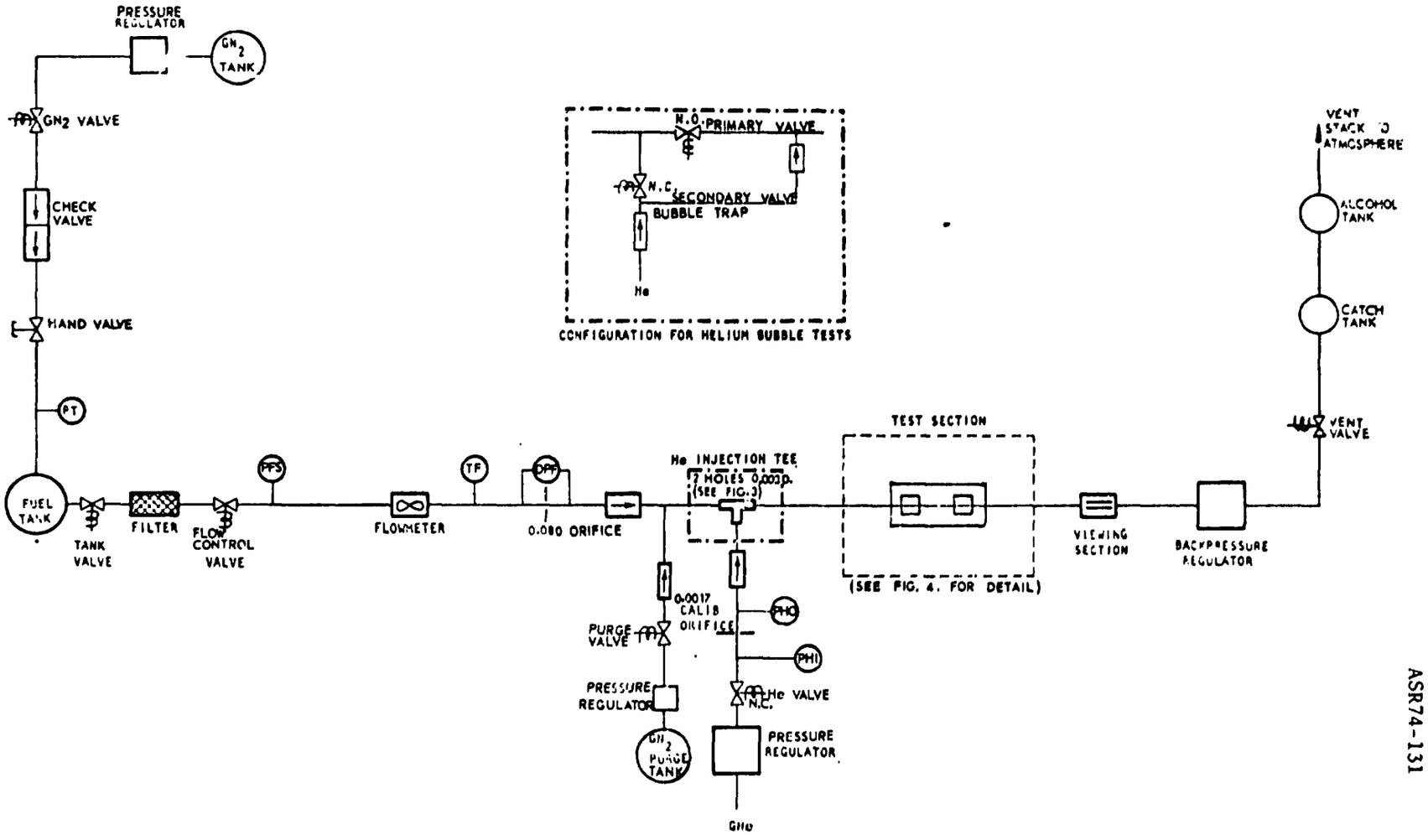

Figure 1. Facility Schematic for Heated Tube Tests

ASR74-131

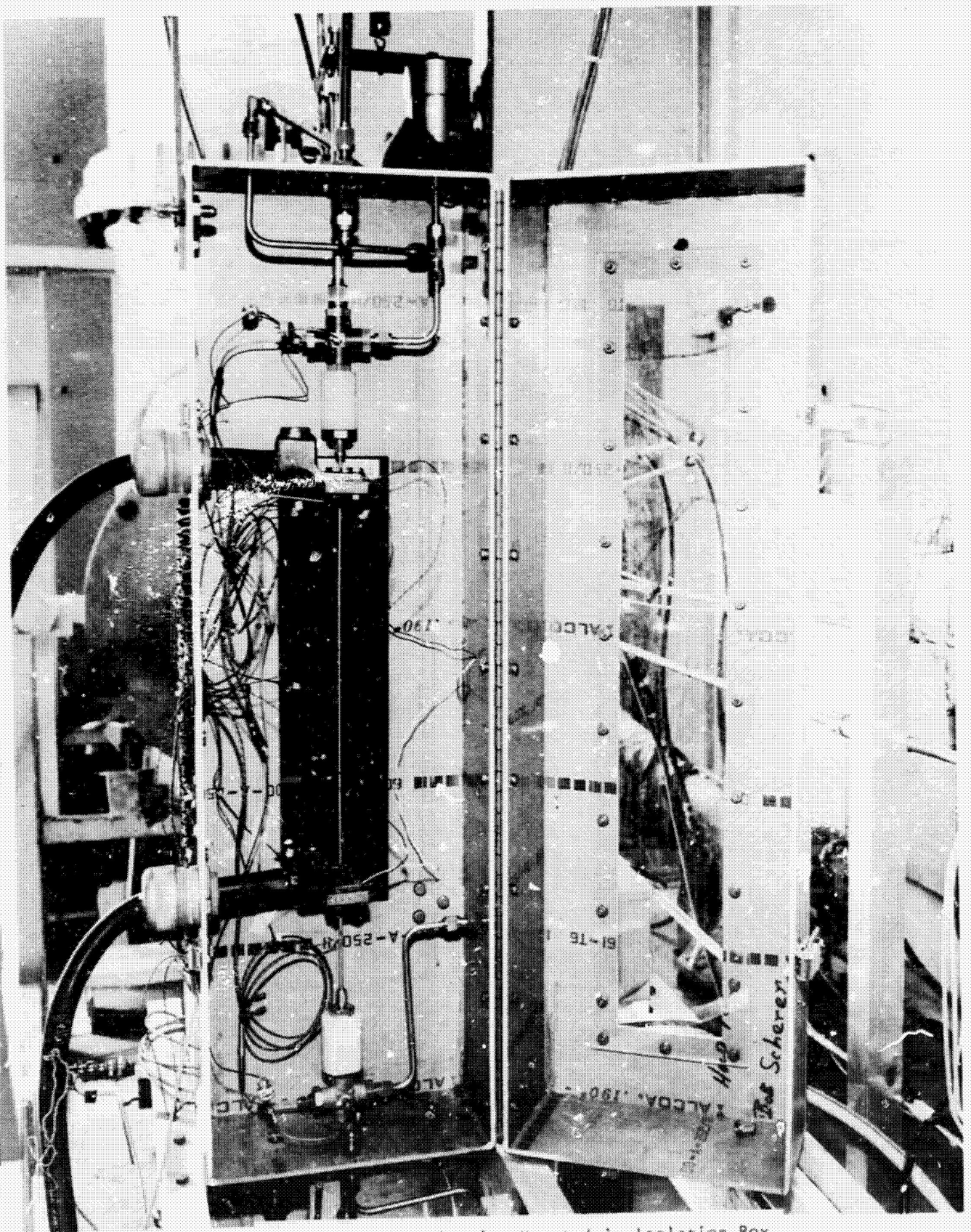

Figure 2. Test Section Mounted in Isolation Box

A GHe system is used for the helium ingestion tests. The system consists of a high-pressure GHe bottle, a regulator, a calibrated flow orifice, and a check valve. The helium system is connected, as shown in Fig. 1, for the helium froth tests. The mixer is a perforated tube sealed in a "T" (Fig. 3) which was located close to the test section to minimize agglomeration of the bubbles.

For the helium bubble tests, the mixer Tee is replaced with the bubble flow circuit shown in Fig. 1. Operation of this circuit is described under TEST PROCEDURES. Essentially, the system provides initial steady-state flow of MMH, followed by injection of a known quantity of helium at nearly constant pressure to accurately simulate flow of a slug of helium through a regeneratively cooled thrust chamber.

Instrumentation parameters, ranges, and display forms are listed in Table 1. A schematic of instrumentation locations is given in Fig. 4.

TEST HARDWARE

Test hardware consisted of both circular tube and rectangular channel assemblies as shown in Figs. 5 and 6, respectively. The hot-start tests utilized 0.25-inch O.D., .18-inch I.D. CRES 321, and electroformed nickel tubes with 4-inch heated length to simulate channel dimensions and materials in the regenerative chamber nozzle region where high temperatures due to nozzle soakback and/or heating is likely to occur. The helium ingestion tests were conducted in 0.125-inch O.D., 0.086-inch I.D. CRES 321 tubes. The nominal heated test section length was 9.6 inches. Copper terminal blocks are brazed to the tubes as shown in Fig. 5 to provide uniform electrical contact around the circumference of the tube. The terminal blocks are mounted to the micarta base, which has slotted holes to allow for thermal expansion.

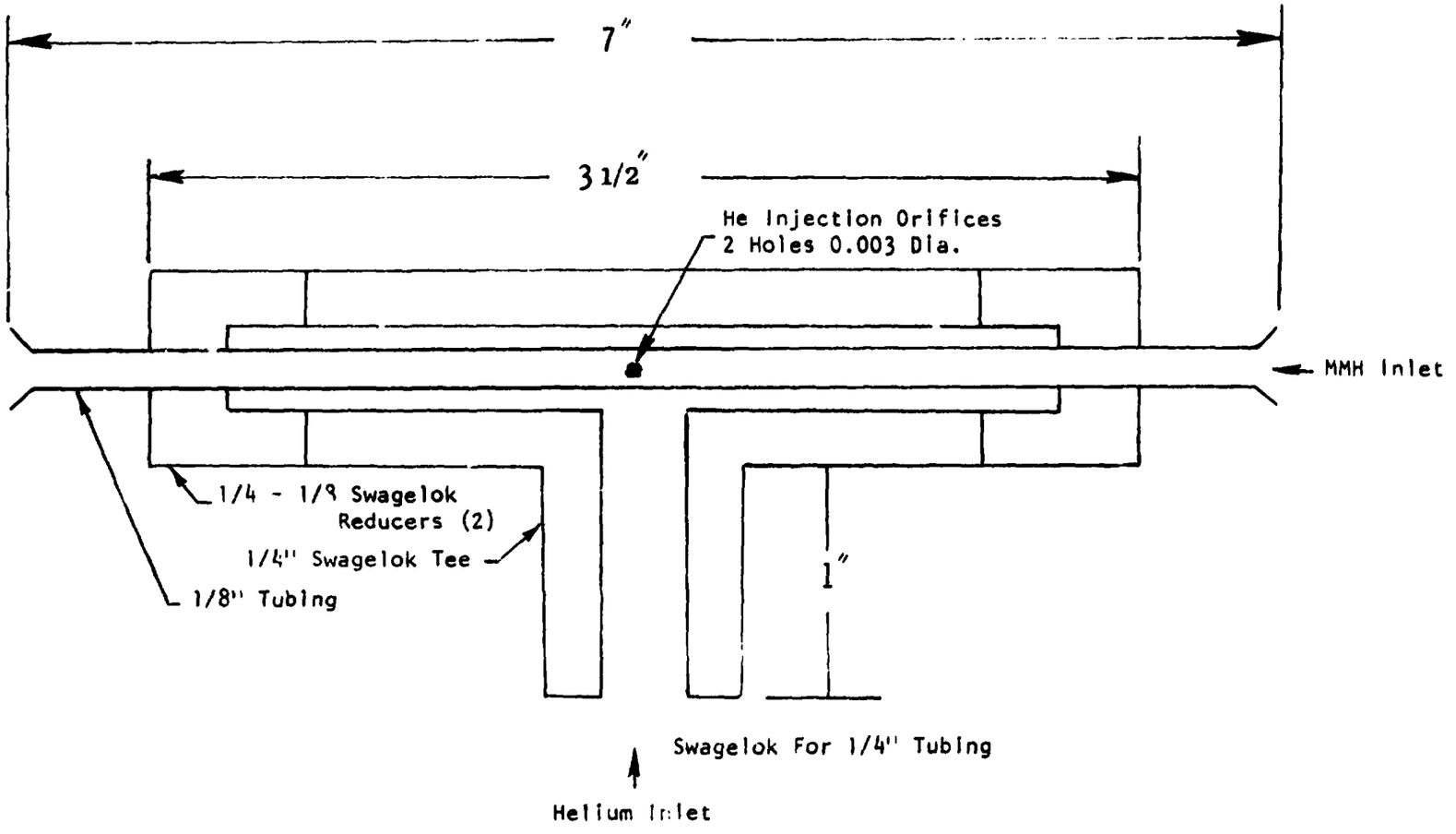

Figure 3. Helium Mixing "T"

TABLE 1

INSTRUMENTATION FOR ELECTRICALLY HEATED TUBE TESTS

Parameter	Symbol	Calibration Range	Display
			O - Oscillograph R - Pen Recorder P - Panel Gage or Meter * - Helium Tests Only
Pressures, psia			
Coolant Orifice Inlet	PFS	0-500	P
Coolant Orifice ΔP	DPF	0-50	O, P
Tube Inlet	PTI	0-500	O
Tube Outlet	PTO	0-500	O, P
GHe Supply	PHS	0-3000	P*
GHe Orifice Inlet	PHI	0-1500	P*
GHe Orifice Outlet	PHO	0-0	P*
Temperatures, F			
Coolant Orifice	TF	0-100	R
Tube ΔT	ΔT	0-500	P
Tube Outlet	TFO	0-500	R
Tube Wall	TW1	0-2000	O
	TW2	0-2000	R
	TW3	0-2000	O
Coolant Flowrate, cps	FC		O
Tube Voltage	V	0-50	O,P
Tube Current, amps	I	0-2000	O, P
Automatic Cutoff, F		500-1500	P
Bubble Valve Signal			P*, O

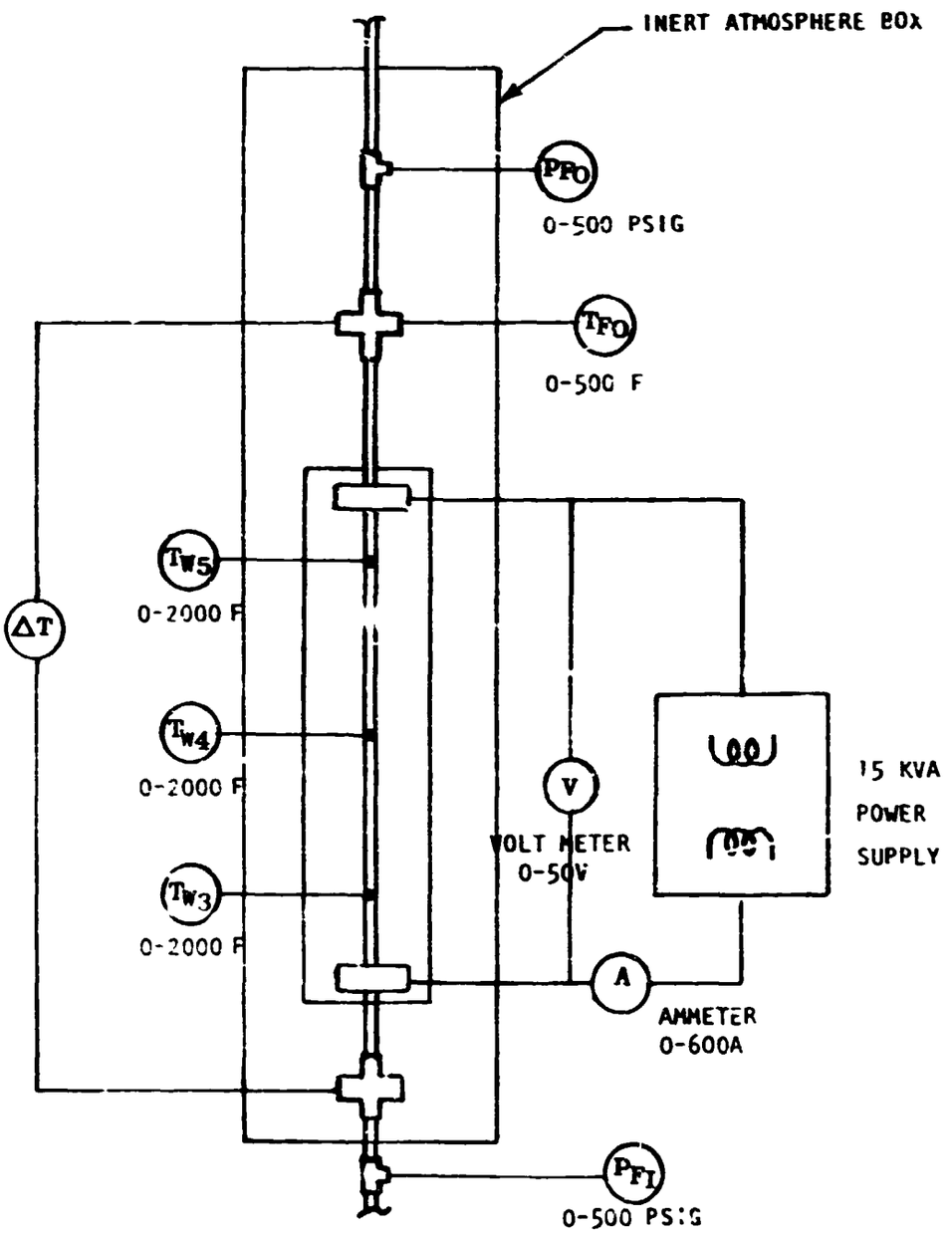

Figure 4. Test Section Power Supply and Instrumentation

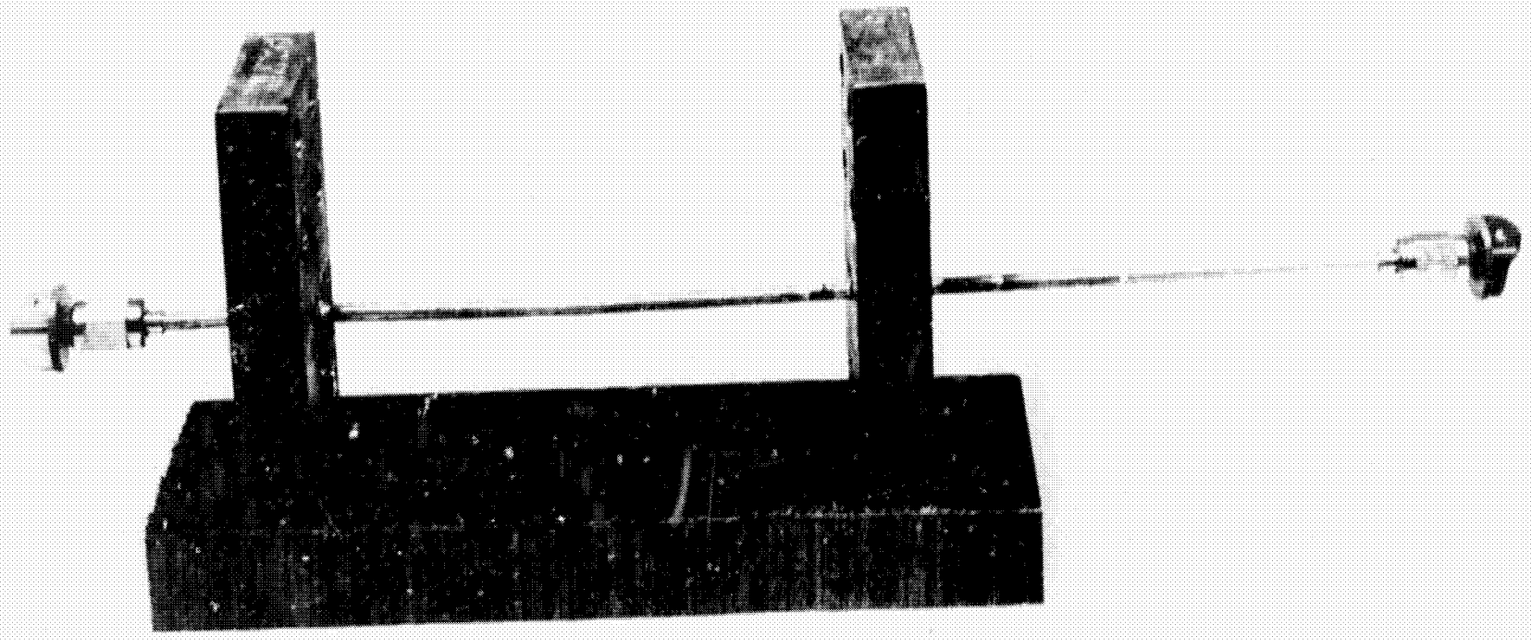

Figure 5. Heated Tube Assembly

Figure 6. 2-D Test Section

The assembly for the two-dimensional heated tube tests consists of a ten-inch rectangular tube onto which circular tube ends are welded for flow connection. A copper strip is brazed to the tube along one surface. Voltage applied to the ends of the strip through the attached copper terminal blocks provides an asymmetric heat input to the tube which simulates heating of the hot wall of the chamber. The nickel close-out is not simulated because the back-wall material has been shown analytically to have little effect on the heat flux distribution in the area of the intersection of the hot wall and land. In addition, a nickel close-out on the test section would affect the electrical heat distribution.

Three copper terminal blocks were brazed to the rectangular test sections to provide for nominal heated lengths of 2, 5, and 7 inches to simulate throat and injector end operating conditions of the regenerative cooled chamber. Three test sections of two different cross-section geometries were fabricated and tested. The pertinent channel dimensions are listed in Fig. 7.

TEST PROCEDURE

Pretest Calibration and Checkout Procedures

The coolant flowmeter was calibrated in water. The coolant flow measuring orifice was calibrated in water and checked against the flowmeter in MMH. A curve of a tank inlet pressure vs flow was generated so that pressures could be set for the hot-start transient tests. The helium flow orifice was calibrated in helium. The quality of the froth and the bubble characteristics were checked by photographing through a glass viewing section. Instrumentation calibrations, in terms of galvonometer deflections for the oscillograph recorder, were checked periodically during the test program.

Figure 7. :ctangular Channel Test Section Geometry

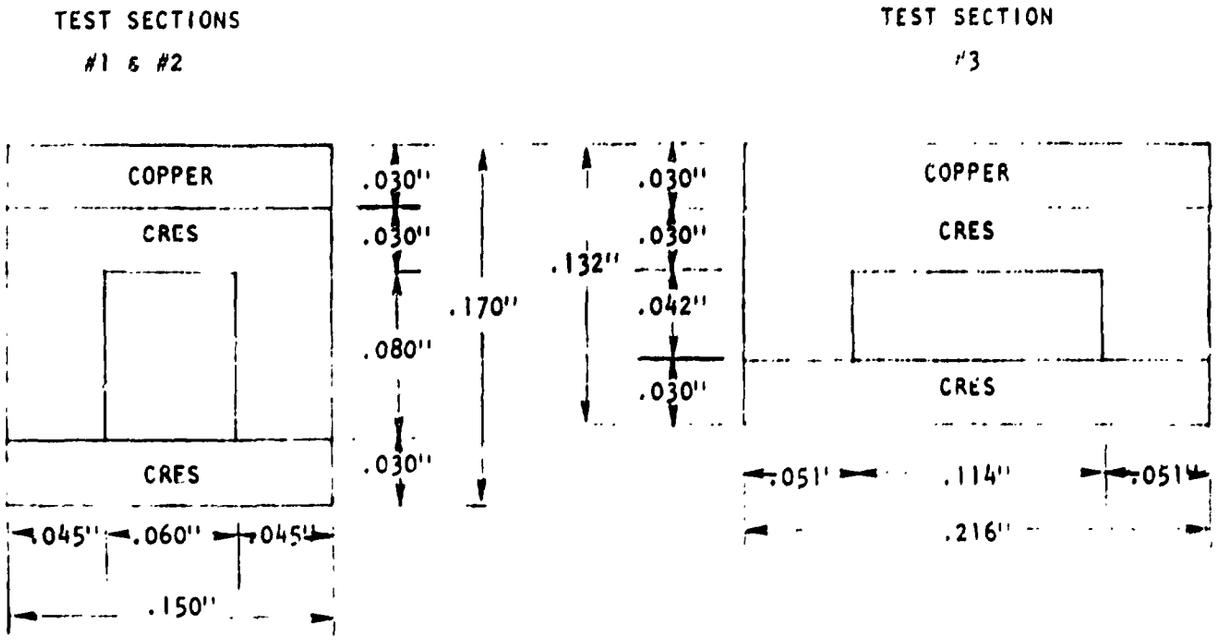

Hot-Start Tests

Prior to each hot-start transient test, the system was purged with GN_2 for approximately five minutes to remove all amine fuel from the system downstream of the run valve. The tank pressure was set for the desired flowrate. The tube was heated slowly by increasing electrical power while monitoring tube wall temperature until the desired temperature level was achieved. The instrumentation and the coolant flow was then turned on for approximately 15 seconds or until sufficient cool-down was achieved. Electric power was turned off followed by coolant flow and finally instrumentation. No back pressure regulator was used during these tests.

Tube temperature levels were increased from 200-300 F to about 1600 F in several steps with decreasing flowrates corresponding to coolant velocities of approximately 10, 7.5, and 5 ft/sec tested at each temperature level.

Helium Bubble Tests

The initial procedure prior to test was to trap a known mass of helium in a secondary flow circuit as shown in the schematic of Fig. 1. This was accomplished by establishing a low-coolant flowrate at a given reduced pressure (by appropriate setting of the tank and back pressure regulators) in the primary flow circuit. Helium was then introduced into the secondary line (of known volume) until the pressure was sufficient to cause the check valve to the primary circuit to open (as verified by helium bubbles in the sight tube). Variations in trapped helium mass were obtained by varying the secondary circuit volume and/or the initial pressure of the system.

The primary coolant pressure was then increased to nominal run condition (although still at low flow). Coolant flow was allowed to bleed into the helium circuit by uncoupling and operating the (normally closed) valve

between primary and secondary line in order to bring the helium pressure up to nearly the same pressure level as the coolant.

The valves in the primary and secondary circuits were recoupled. The coolant flow was then increased to the desired operating level. The charts were turned on and the electrical power increased to a level simulating throat heat flux conditions ($\simeq 2.8$ BTU/in^2-sec). The sight tube motion picture camera was turned on. The two valves were then cycled simultaneously, switching the coolant flow from the primary circuit to the secondary circuit, thereby, forcing the helium bubble through the test section with minimum disruption of flow.

The normal shutdown sequence was: 1) camera off, 2) power off, 3) flow off, 4) charts off.

Helium Froth Tests

The helium pressure was set to provide the desired flowrate across the selected calibrated choked flow orifice (.0017-inches diameter). The desired amine coolant flowrate was initiated and verified. The helium flow was then admitted to the mixing section and the charts turned on. The electric power was gradually increased to the desired injector-end level of about 1.6 BTU/in^2-sec or until a wall temperature excursion occurred in the case of burn-out tests. After power cutoff, the charts were turned off and then the coolant and helium flows were shutoff. A back pressure regulator was used to maintain a pressure of about 180-200 psia at the outlet of the test section.

The froth levels, in general, were increased in successive tests to a maximum value of about 30 percent by volume.

2-D Burn-Out Tests

These tests were conducted by first establishing the desired amine coolant flowrate. The charts were then turned on and the electrical power level gradually increased until a wall temperature increase was noted.

An exception to the above procedure occurred in the first burn-out test, (with 50-50 fuel) wherein there was not sufficient electrical power to cause burn-out at the established flowrate. The flowrate was, therefore, decreased (at maximum electrical power) until a wall temperature excursion occurred. Subsequent tests utilized a larger capacity power source in order to achieve the desired heat flux levels.

DATA ANALYSIS

Hot-Start Tests

The data analysis associated with hot-start tests consisted mainly of verifying the initial test section temperature from the oscillograph and pen recorder charts. In addition, the oscillographs were studied to determine if there were any anomalies in temperature, flow, or pressure traces which might indicate possible fuel decomposition or "popping."

Helium Bubble Tests

The motion pictures of the bubble passing through the downstream sight tube were reviewed to determine bubble duration and quality (i.e., continuous or segmented bubble). The camera speed of 400 frames/second permitted calculation of bubble durations to within about 2 milliseconds accuracy. The oscillographs were reviewed to determine maximum test section temperature resulting from the helium bubble.

Helium Froth Tests

The coolant and helium flowrates were verified from oscillograph orifice pressure drops and flowmeter traces. The corresponding helium volume percent was calculated. The maximum test section wall temperatures and electrical power generation were also obtained from the oscillographs.

In the case of burn-out tests, the electrical power, just before the wall temperature increase, was calculated from the voltage and current traces. The total power divided by the internal surface area of the test tube provided the burn-out heat flux. The coolant outlet temperature and pressure were used to determine outlet subcooling. The velocity of the froth was determined from the measured coolant flowrate and calculated density corresponding to the volume percent of helium. A heat balance of the electrical power input and the coolant enthalpy rise was calculated to determine possible test discrepancies.

1-D Burn-Out tests

The electrical power, coolant outlet temperature and pressure, and coolant flowrate were obtained from the oscillographs at a point just prior to the recorded wall temperature increase indicating transition to film boiling. The outlet temperature and pressure were utilized to determine outlet subcooling. The coolant velocity was calculated from measured coolant flow and known test section flow area.

The asymmetric heat flux equivalent to thrust chamber heating conditions was determined using a two-dimensional thermal conduction model. The analysis technique is discussed in detail in the appendix of this report. The equivalent 1-D heat flux is essentially the total heat generation minus the heat generated in the lands and closeout, divided by the width (lands plus channel) of the test section. In general, this heat flux level is about 13 percent lower than if it were assumed that all of the

heat generation occurred in the copper strip and none in the CRES section.

TEST RESULTS

Hot-Start Tests

A total of 44 hot-start simulation tests were conducted. A brief overall test summary is given in Table 2. The individual test conditions and results are summarized in Tables 3 and 4. Tube temperatures as hot as 1600 F were attained with both CRES and nickel tubes with flows as low as half of the anticipated engine start value. In all cases, the tube wall temperatures (temperatures were recorded at two axial locations on the tubes) decayed with no indication of overshoot. Pressure traces indicated that no "popping" occurred, although some low frequency (50 cps) low amplitude (15 psi peak-to-peak) oscillations were occasionally recorded. The fluctuations were harmless and probably resulted because of the low pressure at which the tubes were operated to approximate pressures which would exist in the engine during a vacuum start.

A typical oscillograph record is shown in Fig. 8 for a 1600 F test on the nickel tube. The rise of tube inlet pressure is indicative of the time at which the coolant entered the tube. However, the heated portion of the tube begins about 5 inches downstream of the inlet pressure tap so that the coolant enters the heated portion of the tube approximately 0.05 seconds later. Both wall temperatures begin to decay very soon after coolant reaches the hot tube, although the upstream temperature initially decays at a much more rapid rate indicating the possibility of nucleate boiling transitioning to film boiling along the length of the tube. The subsequent increasing rate of temperature decay in the downstream region could indicate a change from film to nucleate boiling at a sufficiently low wall temperature.

TABLE 2

HOT-START TEST SUMMARY

- MMH Test Summary
  - 20 Tests With CRES Tubes
    - 190°F to 1610°F Tube Temperatures
    - 5 to 10 ft/sec Velocity
  - 9 Tests With Electroformed Nickel Tube
    - 310 to 1590°F Tube Temperatures
    - 5 to 10 ft/sec Velocity
- Immediate Quench For All Tests
- 50-50 Test Summary
  - 8 Tests With CRES Tubes
    - 750 to 1620 F Tube Temperatures
    - 5 to 10 ft/sec Velocity
  - 7 Tests With Electroformed Nickel Tube
    - 646 to 1620 F Tube Temperature
    - 5 to 10 ft/sec Velocity
- Immediate Quench For All Tests

TABLE 3

OME HOT-START SIMULATION TESTS WITH MMH

Test	Tube Material	Initial Temp, F	Coolant Vel. (ft/sec)	Remarks
1-1	CRES No. 1	190	10	Quenched without temperature overshoot
1-2		280		
1-3		300		
1-4		630		
1-5		1000		
1-6		1200		
1-7		1340		
1-8		1200		
1-9		1070		
1-10		70		
1-11		1500		
1-12		1610		
1-13	CRES No. 2	620	8	
1-14		980		
1-15		1210		
1-16		1590		
1-17		600	5	
1-18		1030		
1-19		1210		
1-20		1600		
1-21	Electroformed Nickel	310	10	
1-22		890		
1-23		1130		
1-24		1580		
1-25		800	8	
1-26		1580	8	
1-27		350	5	
1-28		810	5	
1-29		1590	5	

NOTES: Tube dimensions = 0.25" O.D. X0.035" wall X 4.0"

No. 1 and No. 2 are identical samples.

TABLE 4

OME HOT-START SIMULATION TESTS WITH 50-50

Test	Tube Material	Initial Temp, F	Coolant Vel. (ft/sec)	Remarks
1-83	CRES No. 1	750	10	Quenched without temperature overshoot
1-84	↓	1020	10	↓
1-85		1280	10	
1-86		1625	10	
1-87		1260	8	
1-88		1620	8	
1-89		1310	5	
1-90	↓	1610	5	
1-91	Electroform. Nickel	646	10	
1-92	↓	1220	10	
1-93		1600	10	
1-94		1115	8	
1-95		1600	8	
1-96		1200	5	
1-97	↓	1620	5	↓

FOLDOUT FRAME

REPRODUCIBILITY OF THE ORIGINAL PAGE IS POOR

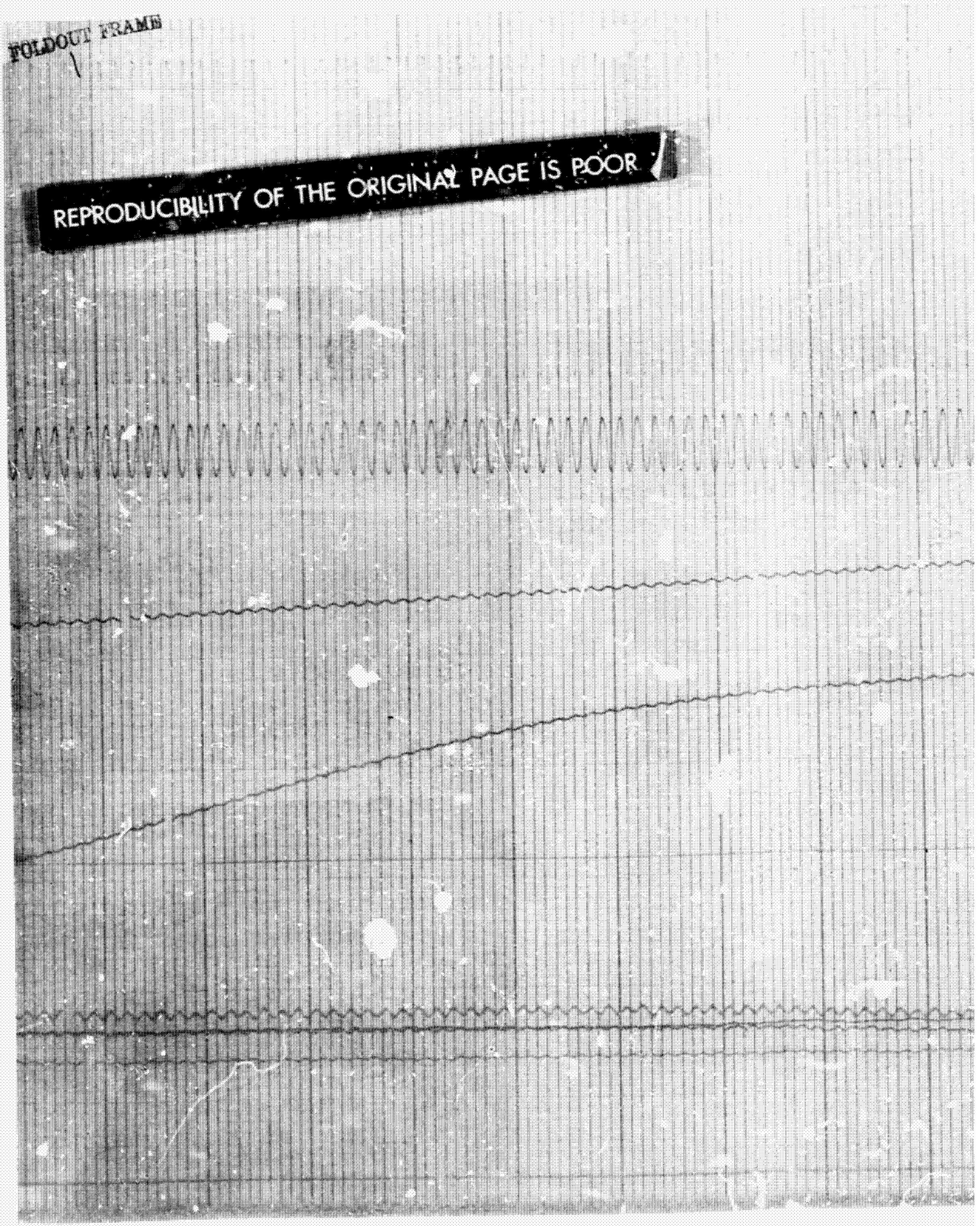

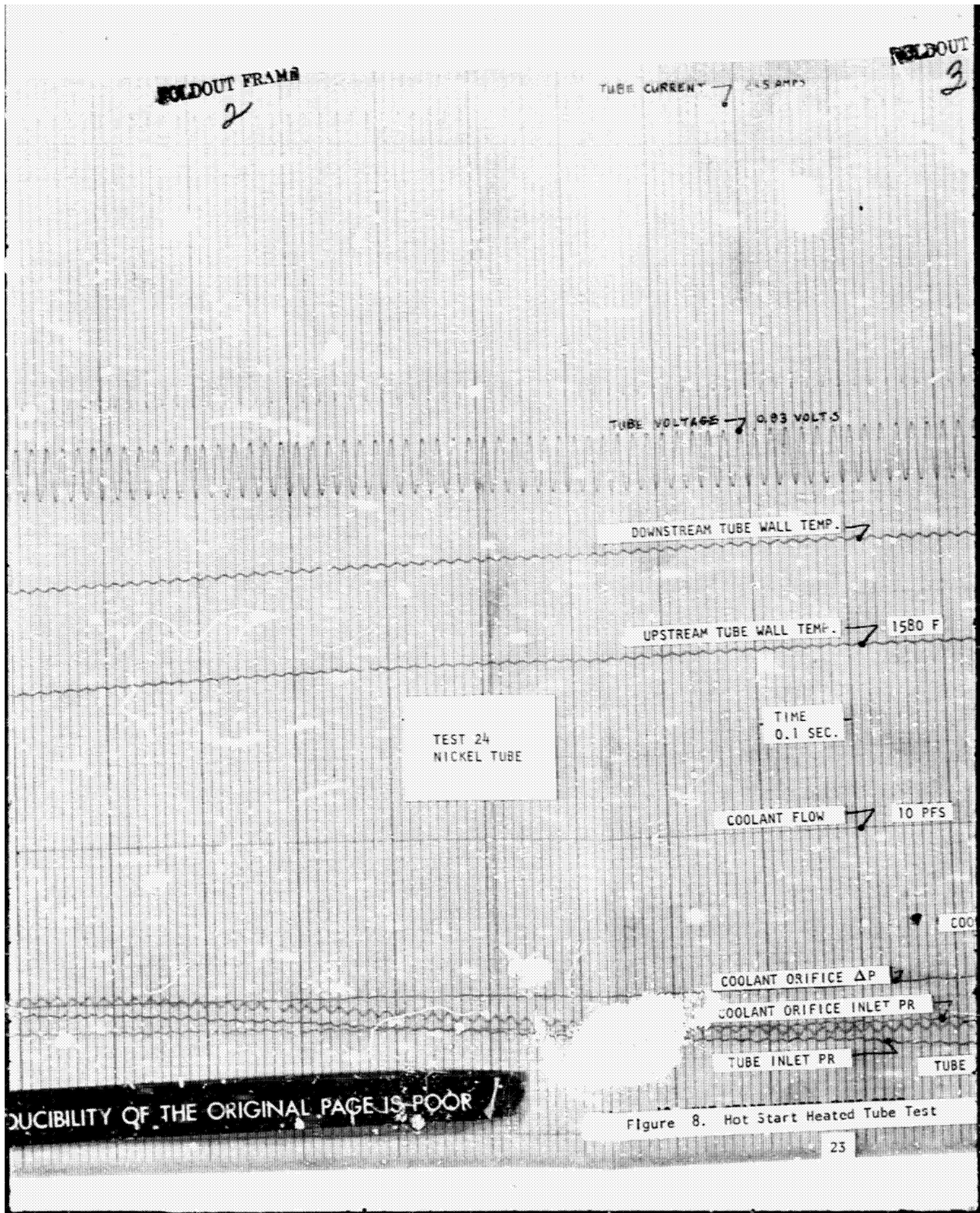

Figure 8. Hot Start Heated Tube Test

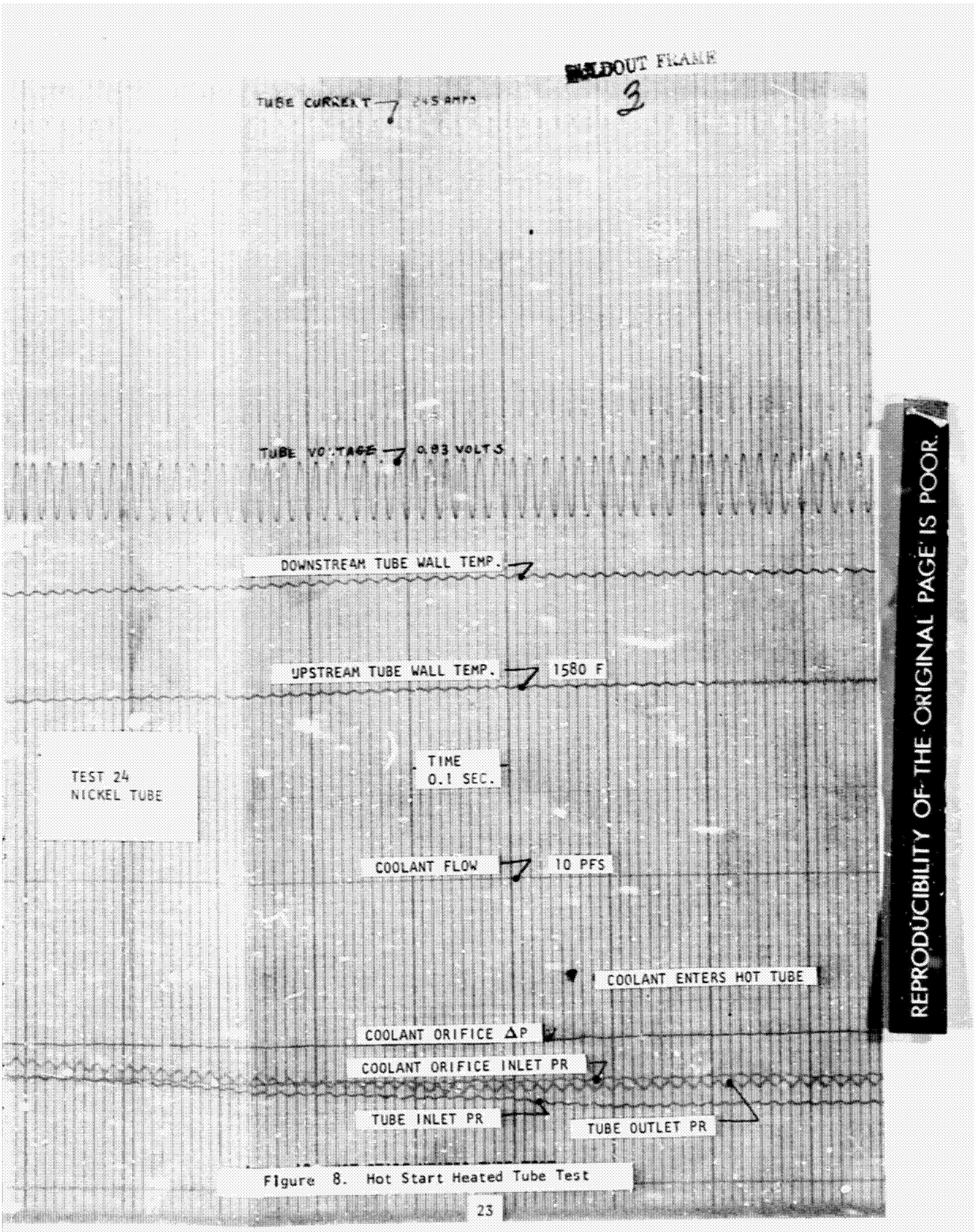

Figure 8. Hot Start Heated Tube Test

Based on the results of this test series, it appears that the anticipated temperatures to which the OME thrust chamber will be heated prior to start will impose no limits or have any adverse effects on regenerative cooling with either MMH or 50-50.

Helium Bubble Tests

A total of 82 helium bubble ingestion tests were conducted with MMH and 50-50 coolants. Fifty-three of the tests utilized circular CRES or nickel tubes and the remaining twenty-nine were conducted with asymmetrically heated rectangular channel CRES test sections. The purpose of these tests was to simulate a bubble of helium tank pressurant passing through the maximum heat flux region of the throat with the regenerative fuel coolant in the event of a screen failure in a fuel tank. The throat region is believed to be the most critical in regards to helium bubble sensitivity since the higher heat flux level will result in a faster wall temperature rise rate than at the injector end. Bubbles of various sizes were injected to determine what duration the tube wall could tolerate and the ability of the coolant to quench the rising wall temperature without decomposition and/or detonation. Figure 9 depicts a typical bubble as seen from a sight tube located downstream of the test section.

Two CRES 347 tubes were operated at heat fluxes from 2.0 to 4.6 BTU/in^2-sec with a nominal coolant velocity of 22.5 ft/sec. The 2-D CRES test sections were operated at corrected (see Appendix) heat flux levels from 2.5 to 3.2 BTU/in^2-sec at nominal coolant velocities of about 22 and 40 ft/sec. The 2-D model cross-section geometry actually simulates the chamber injector end geometry since these test sections were built primarily to evaluate burn-out limits at injector-end conditions. A second buss bar added to these test sections (resulting in a 2-inch heated length) permitted testing at the higher heat flux and lower bulk temperature associated with throat conditions. The larger mass ($\simeq$70%) of this test section would tend to have a lower temperature response than an actual throat section geometry although this is somewhat compensated for by the increased heated surface area.

The tubular test results are summarized in Table 5 and the channel test results in Table 6. A graphical presentation of all of the tests in terms of bubble duration and heat flux is depicted in Fig. 10.

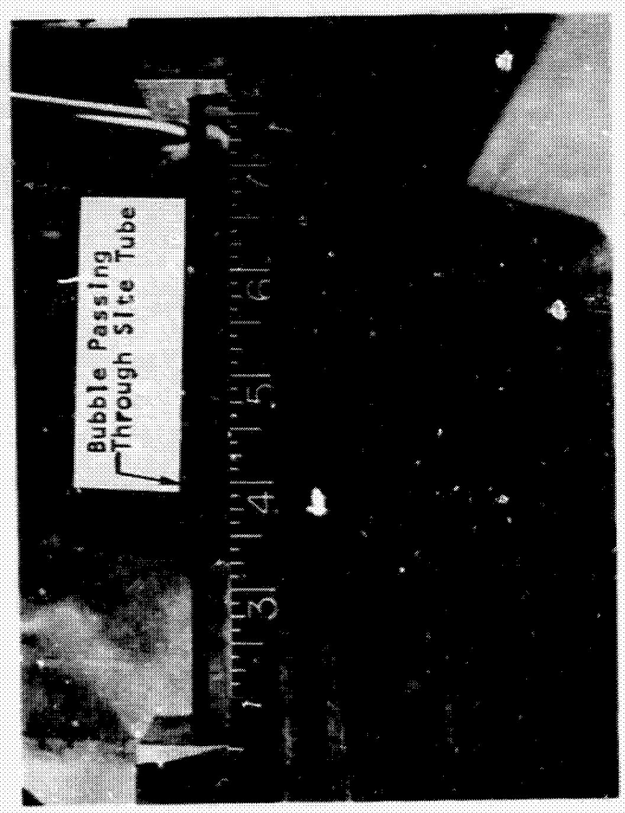

Figure 9. Typical Bubble Test

Table 5. [illegible] Bubble Injection Test Summary - Circular Tube Test Section

1 TEST NO.	2 COOLANT	3 CRES* TUBE HEATED LENGTH, IN.	4 COOLANT FLOWRATE, LB/SEC	5 HEAT FLUX, BTU/HR-FT²-SEC	6 BUBBLE INJECTION SEC	7 COOLANT INLET TEMP, F	8 ** COOLANT OUTLET TEMP, F	9 COOLANT OUTLET PRESSURE PSIG	10 COOLANT VELOCITY FT/SEC	11 COOLANT OUTLET SUB-COOLING F	12 OUTLET ΔT_{SUB} FT-F/SEC	13 14 15 REMARKS
1-30	50%	4.0	.072	2.0	.017	73	122	≈150	22.5	241	5430	
31				3.35	.017	74	155			208	4690	
32				4.65	.017	74	187			176	3970	T_{wi} >1800F Burnout
33				3.25	.017	76	155			208	4690	
34				3.36	.034	76	133			230	5180	
35				3.05	.046	70	144			219	4930	
36				2.37	.051	70	128			235	5290	
37				3.05	-	71	145			218	4910	
38				3.98	.051	71	146			217	4890	
39				2.39	.028	71	129			234	5270	
40				3.08	.028	71	146			217	4890	
41				2.39	.080	72	130			233	5250	
42				3.09	.081	72	147			216	4870	T_{wi} >2000F Both ends
43				2.69	.081	73	138			225	5070	
44				2.84	.081	73	143			220	4960	
45				3.05	.081	73	148			215	4840	
46				3.12	.098	73	149			214	4820	80F T_{wi} Rise
37				3.12	.13	73	149			214	4820	One inch red
48				3.15	.13	73	150			213	4800	40F T_{wi} rise
49				3.15	.13	74	151			212	4780	20F T_{wi} rise
50		2.0		3.08	.007	71	109			254	5720	
51				3.10	.018	72	110			253	5690	
52				3.12	.044	72	110			253	5690	One inch red near outlet
53				3.06	.037	72	109			254	5720	
54				3.06	.044	72	109			254	5720	
55				3.04	.044	72	109			254	5720	
56				3.04	.044	72	109			254	5720	
57				3.04	.060	72	109			254	5720	
58				3.57	.008	74	117			246	5540	
59				3.57	.018	74	117			246	5540	
60				3.57	.024	73	116			247	5560	
61				3.57	.037	74	117			246	5540	
62				3.57	.041	74	117			246	5540	
63				3.59	.059	74	118			245	5520	
64				3.57	.060	74	117			246	5540	
65				3.57	.062	74	117			246	5540	
66	SAT. H2O			3.03	.007	72	109			254	5720	
67				3.03	.015	72	109			254	5720	
68				3.04	.024	72	109			254	5720	
69				3.04	.037	72	109			254	5720	
70				3.04	.041	72	109			254	5720	
71				3.04	.060	72	109			254	5720	
72				3.04	.072	72	109			254	5720	
73				3.04	.084	72	109			254	5720	
74				3.03	.12	72	109			254	5720	
75				3.04	.20	72	109			254	5720	
76	50-50		.074	3.11	.008	72	109			244	5490	
77				2.31	.008	71	98			255	5740	
78				3.04	.008	71	107			246	5540	
79				3.10	.008	71	108			245	5510	
80				3.10	.035	71	108			245	5510	
81				3.10	.072	71	108			245	5510	
82				3.11	.20	71	108			245	5510	One inch red near outlet

* CRES TUBE DIMENSIONS - .134 IN. O.D. x .014 IN. WALL

** CALCULATED FROM HEAT INPUT

Table 6. Helium Bubble Ingestion Test Summary - Rectangular Channel Test Section

ASR74-131

	1 Test No.	2 Coolant	3 *Test Section	4 Coolant Flowrate (lb/Sec)	5 **Heat Flux $\frac{BTU}{(in^2-sec)}$	6 Bubble Duration (Sec)	7 Coolant Inlet Temp. (F)	8 *** Coolant Outlet Temp. (F)	9 Coolant Outlet Pressure (psig)	10 Coolant Velocity (ft/sec)	11 Coolant Outlet Subcooling (F)	12 Outlet $V \cdot \Delta T_{sub}$ $\frac{Ft-F}{Sec}$	13	14 REMARKS	15	16
1	1-98	50-50	#1	.038	2.62	-	71	104	180	21	259	5440				
2	99				2.60	.035	71	104			259	5440				
3	100				2.64	.10	71	105			258	5420				
4	101				2.60	.10	72	105			258	5420				
5	102				2.62	.15	72	105			258	5420				
6	103				2.64	.23	72	106			257	5400				
7	104				2.63	.25	72	106			257	5400				
8	105				3.24	.26	72	113			250	5250				
9	106				3.26	.28	70	111			252	5290				
10	107				3.24	.28	70	111			252	5290				
11	2-33	HHH	#2	.073	2.74	0 (Froth)	63	81	180-190	42	284	12000				
12	34				2.74	0 (Froth)	63	81			284	12000				
13	35				2.78	.025	63	81			284	12000				
14	36				2.73	.04	64	82			283	11900				
15	37				2.82	.15	64	83			282	11900				
16	38				2.77	.25	64	82			283	11900				
17	39				2.77	.31	64	82			283	11900				
18	40				2.73	.20	65	83			282	11900				
19	41				2.75	.25	65	83			282	11900				
20	42				2.76	.28	64	82	192		287	12100		55 F wall temp. rise		
21	43			.077	2.77	.37	65	82	180	44	281	12400		50 F wall temp. rise		
22	44			.076	2.75	.29	66	82	180	44	281	12400		35 F wall temp. rise		
23	51		#3	.038	2.83	.59	58	110	150-160	21	240	5030				
24	52				2.58	.78		105			245	5140				
25	53				2.58	.89		105			245	5140				
26	54				2.58	1.05		105			245	5140				
27	55				2.58	1.24		105	154		244	5130		320 F wall temp. rise		
28	56				2.57	1.15		105	164		250	5250		320 F wall temp. rise		
29	57				2.57	1.10	55	102	160		251	5260		320 F wall temp. rise		
30																
31																
32																
33	*Heated Length = 2.0 Inches (See Fig. 7 for Dimensions)															
34	** Adjusted Down by 13 Percent to Account for Heat Generation in Lands and Closeout															
35	*** Calculated Based on Heat Input															

FOLDOUT FRAME

FOLDOUT FRAME

ASR74-131

Figure 10. Helium Bubble Ingestion Test Operating Map

From the graphical representation of the tests, it can be seen that only five of the 82 tests exhibited overheating similar to a burn-out phenomena. All five of these tests occurred in the circular tube test sections at bubble durations considerably below that achieved in the 2-D channel test sections. One of the tests (#1-32) was a sufficiently high heat flux (4.6 BTU/in^2-sec) as to be on the verge of transition to film boiling (based on previous data) even without a helium bubble. This test is, therefore, not representative. Three of the remaining tests indicating burn-out were with MMH coolant. Test 1-32 glowed red during test, but self-quenched. Test 1-42 would probably have burned out the tube had the power not been cut manually. The tube wall temperature trace shows a 1000 F rise in 0.6 seconds, prior to cut-off, at both ends and center of the tube. This occurred with a bubble duration of about 0.081 seconds at a heat flux of 3.09 BTU/in^2-sec. The tube exceeded 2000 F again on Test 1-52 with 0.044 sec bubble at 3.12 BTU/in^2-sec. This was the shortest duration in which burn-out was indicated with MMH. For both of these cases, the wall temperatures continued to rise even after the liquid coolant re-entered the test section. Efforts to reproduce these results on successive tests failed. Tests with helium saturated MMH indicated no sign of wall temperature rise with bubbles up to 0.2 seconds in duration.

Test 1-82 with 50-50 as coolant was cutoff with a wall temperature near the outlet above 2000 F with a heat flux of 3.11 BTU/in^2-sec and bubble duration of about 0.2 sec. All other tests showed at most a few degrees temperature rise as the bubble passed through the test section.

Testing with 50-50 in the 2-D channel was conducted without incident in the initial test program (Test 1-98 to 1-107) at bubble durations up to 0.28 sec. In the second test program, testing in 2-D channel sections continued utilizing MMH coolant. The maximum bubble duration of about 1.2 sec occurred in Test 2-55 at a nominal corrected heat flux of

2.6 BTU/in^2-sec and a velocity of 22 ft/sec.

The oscillograph traces for Test 2-55 are presented in Fig. 11. The point in time at which the bubble passes through the test section can be obtained from the test section inlet pressure trace. The reduced helium density results in reduced test section inlet pressure. The outlet pressure is maintained constant (except for an initial transient) by the back pressure regulator. The estimated bubble duration based on the pressure trace is about 1.1 sec, which compares favorably with the 1.2 sec obtained by a frame count of the sight tube motion pictures.

The two test section wall temperature measurements are seen to ramp upward soon after the bubble enters the test section. These temperatures are measured on the CRES sides of the test section as close as possible (≈0.010 - 0.015 inch) to the CRES-copper interface. The temperatures peak out at about 1000 F (compared to nominal operating levels of 640-680 F), approximately 0.5 - 0.7 sec after the bubble passes through the test section. The continuing temperature rise after the bubble exits is probably due to the trailing froth which was apparent in the motion pictures. Self-quenching occurred in this case as it did in all cases conducted with the rectangular test sections.

The capability of the 2-D channel section to absorb longer bubble durations than the circular tubes without excessive temperature excursions is believed due to the larger mass and non-uniform heating. In the channel section, the CRES, closeout is relatively cold (~100-200 F) during normal operation. As the bubble passes through and the electrically heated surface temperature begins to rise, considerable heat is conducted to the cold lands and close-out. In essence, the average temperature and thermal response of the rectangular channel section are lower than for the uniformly heated thin-wall circular tube.

FOLDOUT FRAME

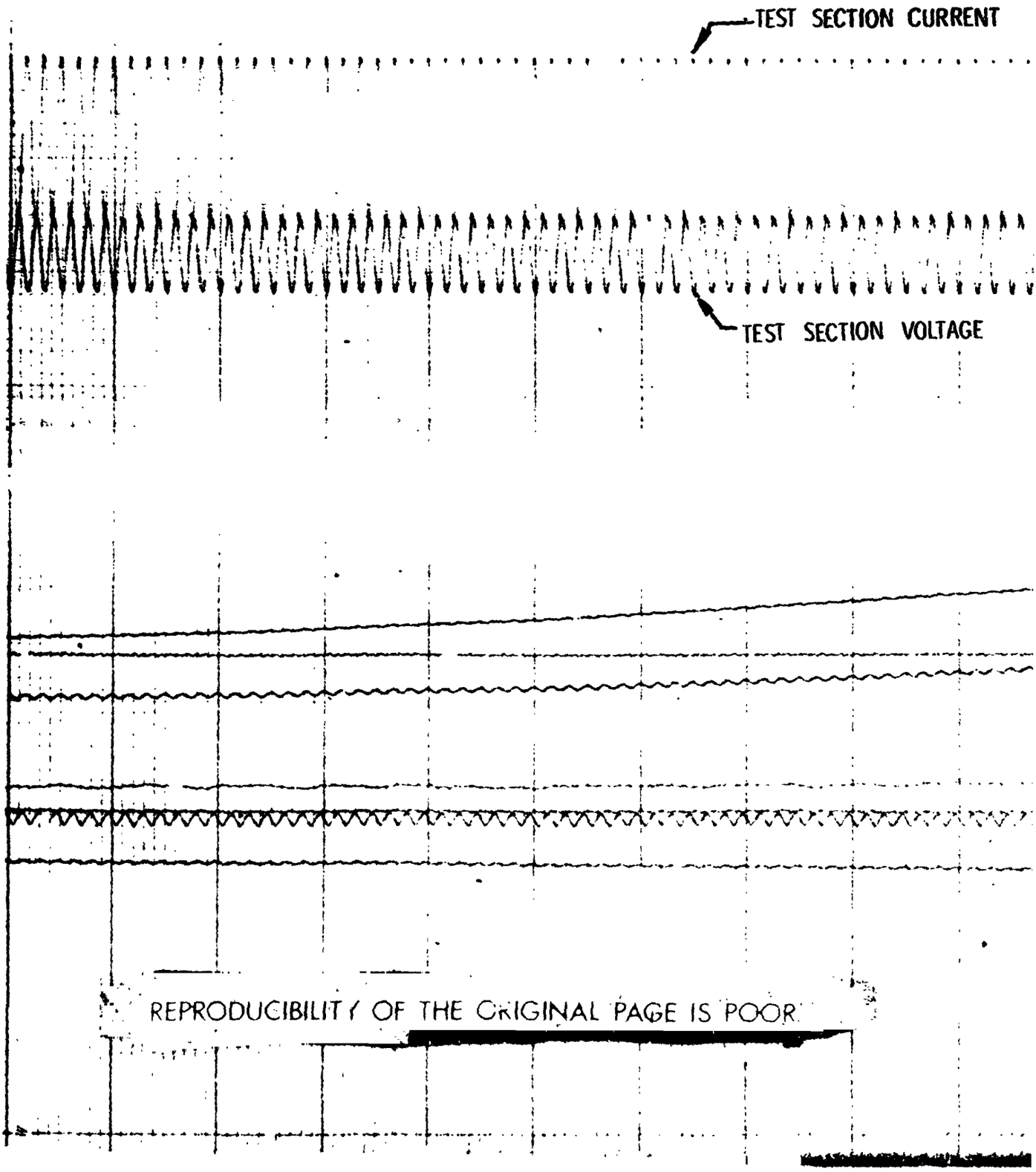

FOLDOUT FRAME

2

FIGURE 11

OSCILLOGRAPH OF HE
BUBBLE TEST #2-5

ENT

GE

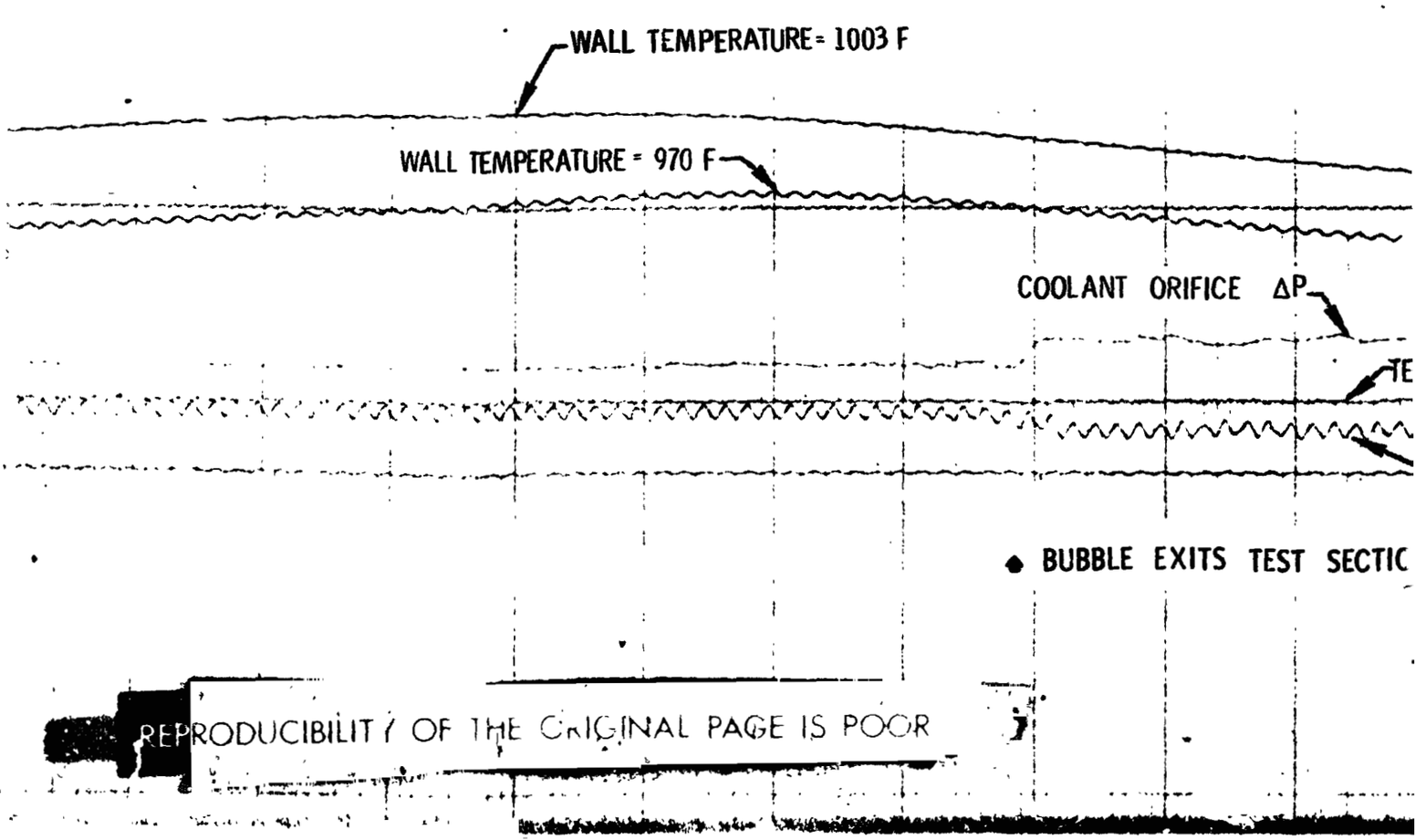

. 11

OF HELIUM

T #2-55

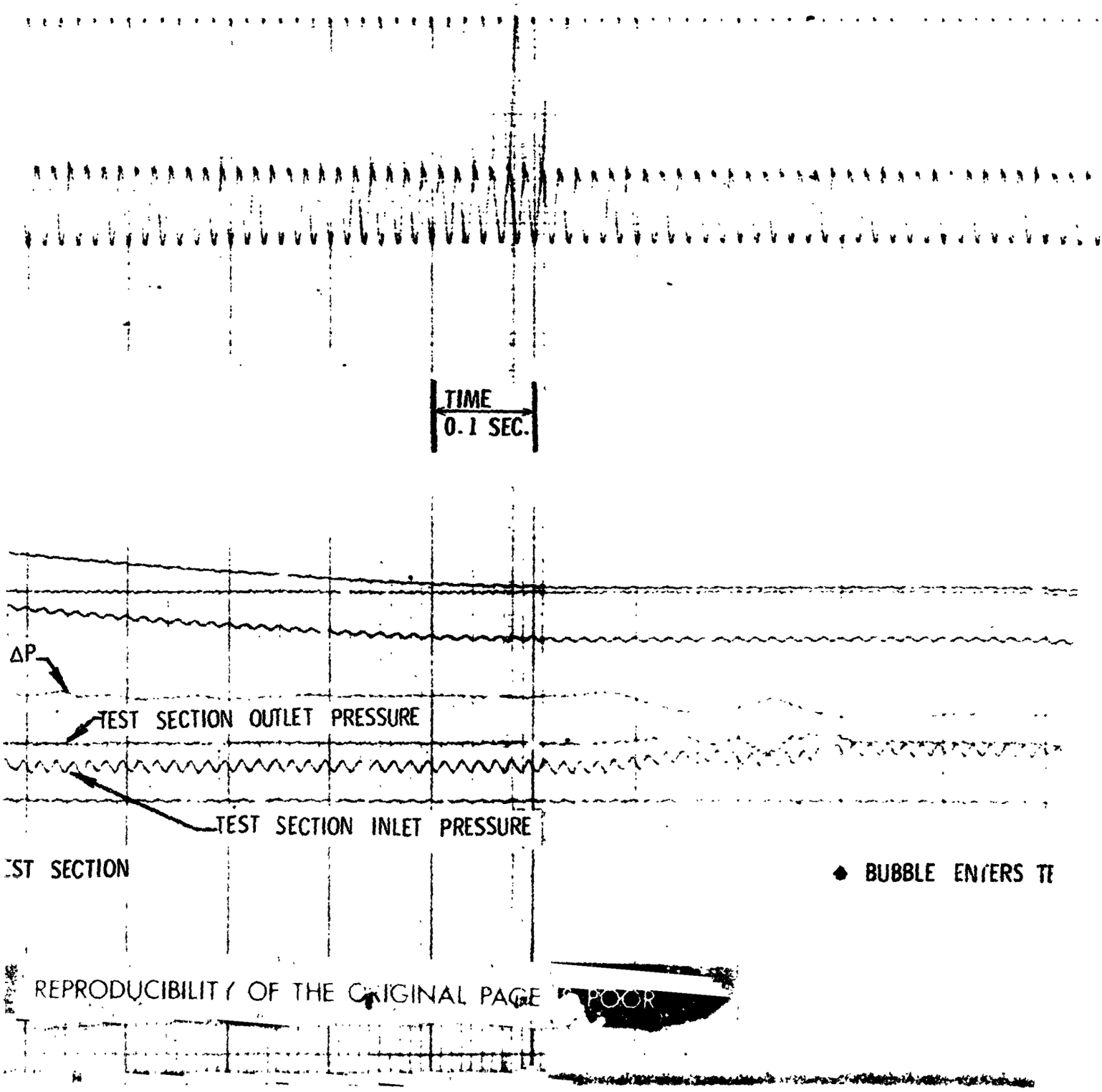

BLOWOUT FRAME
4

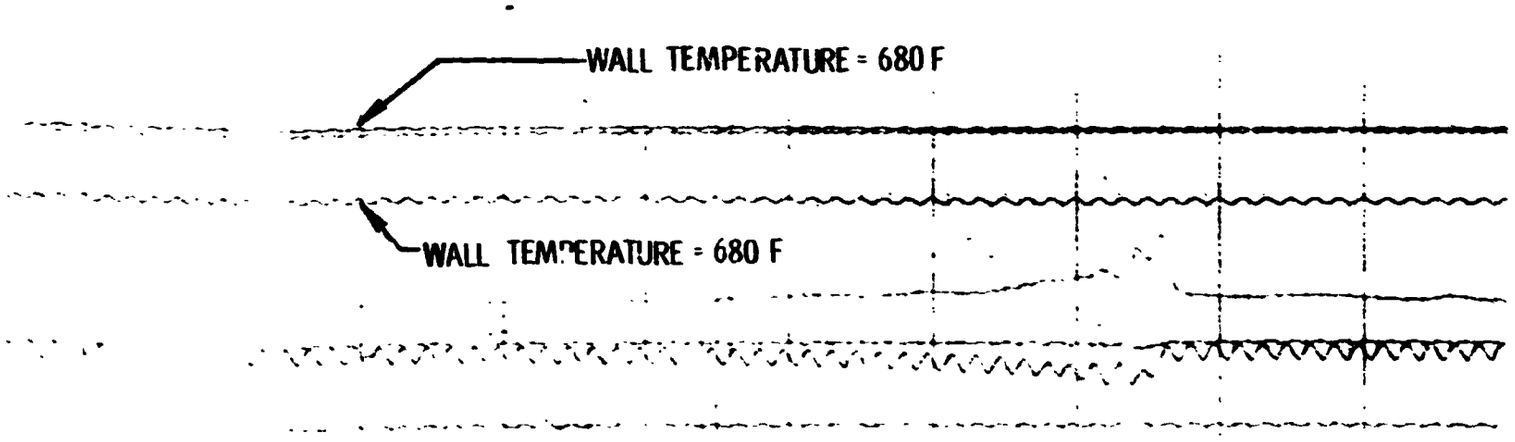

◆ VALVES SWITCHED

ERS TEST SECTION

Helium Froth Tests

A total of 18 tests were conducted in the helium froth test series utilizing uniformly heated circular tube test sections. These tests consisted of 8 tests with 50-50 coolant and 10 tests with MMH coolant. The helium flow ranged from slightly greater than zero to about 30 percent by volume of the total flow through the circular tube test section. These tests are summarized in Table 7.

Photographs of the MMH flow with various amounts of helium are presented in Fig. 12. These pictures were taken of the horizontal sight tube located downstream of the vertical test section.

The purpose of these tests was two-fold: 1) determine whether the test section could accept helium froth flow at conditions simulating OME injector-end operation and, 2) establish the effect of helium froth on the burn-out limit of the amine fuels. The injector end region is believed to be the most critical in terms of helium froth sensitivity since the relatively high coolant temperature and low subcooling would seem to make transition to film boiling highly susceptible to changes in coolant flow conditions.

The nominal test operating conditions in terms of coolant velocity, outlet subcooling, and heat flux level were intended to simulate injector-end values for the Rocketdyne OME Integrated Thrust Chamber (ITC) design which is regeneratively cooled with MMH. These nominal design values are 25-30 ft/sec coolant velocity (without helium), 130°F subcooling and about 1.8 BTU/in^2-sec heat flux level. The appropriate coolant flowrate and electrical power were selected based on a supposed CRES tube with an inner diameter of 0.069 inches. Posttest sectioning and measurement of the tubular test sections indicated a tube inner diameter of 0.086 inches due to a wall thickness of about 0.020 inches rather than the specified value of 0.028 inches. The resultant experimental adjusted heat flux and

TABLE 7. HELIUM FROTH TEST RESULTS

	Test No.	Coolant	Test Section	Froth Percent Helium / Inlet	Froth Percent Helium / Outlet	Coolant Flowrate (lb/sec)	Heat Flux BTU / In²Sec	Coolant Inlet Temp. (F)	Coolant Temp. Rise (F)	Coolant Outlet Temp. (F)	Coolant Outlet Pressure (psig)	Froth Velocity (Ft/Sec)	Outlet Subcooling T_{SUB} (F)	$V \cdot \Delta T_{SUB}$ Ft·°F / Sec	Heat Balance = $1 - \frac{Q_{out}}{Q_{in}}$ (Percent)		Remarks
1																	
2	2-11	50/50	#1 Tube	13.6	15.1	.0280	1.52	59	172	231	182	15.7	123	1930	12		
3	2-12			19.6	21.5	.0290	1.47	62	161	223	179	16.5	120	2130	15		
4	2-13			29.8	32.7	.0280	1.50	60	169	229	174	17.9	121	2170	13		
5	2-14			19.7	21.9	.0278	1.52	61	168	229	182	16.4	125	2050	15		
6	2-15			13.4	15.5	.0275	1.52	60	168	228	173	15.5	121	1880	16		
7	2-16			4.5	4.88	.0280	1.53	60	168	228	174	15.9	122	1700	15		
8	2-17			9.7	9.82	.0275	1.52	60	166	226	190	14.7	131	1930	12		
9	2-18			31.0	37.5	.0262	2.28	62	244	306	172	16.9	43	730	19	Burned	Tube Ruptured
10																	
11	2-19	50/50	#2 Tube	5.1	5.35	.0275	1.56	57	180	237	184	14.1	136	1920	12		
12	2-20			10.0	10.9	.0265	1.55	60	181	241	184	14.6	132	1930	14		
13	2-21			14.0	15.4	.027	1.56	60	186	246	≈180-190	15.6	127	1980	11		
14	2-22			20.2	22.-	.027	1.55	59	178	237	≈180-190	16.4	136	2230	14		
15	2-23			27.3	29.3	.027	1.55	58	180	238	≈180-190	16.9	135	2280	13		
16	2-24			29.1	31.3	.027	1.55	57	183	240	195	17.9	138	2170	11		
17	2-25			30.5	35.0	.0269	1.79	57	209	266	182	17.8	106	1890	13	Transit	to Film Boiling
18	2-26			29.1	33.3	.0270	1.74	59	208	267	186	17.9	107	1920	11	Transition to Film Boiling	
19	2-27			14.8	19.0	.0255	1.81	60	231	291	186	14.7	83	1220	10	Transit	n to Film Boiling
20																	
21	2-67			4.2	5.76	.0340	1.69	67	190	257	158	17.4	103	1790	5	Transit	to Film Boiling
22																	
23																	
24																	
25																	
26																	
27																	
28																	
29																	
30																	
31	NOTES: Tube I.D. = .086 inches, heated length = 9.4 inches.																
32	No. 1 and 2 tubes are identical.																
33																	
34																	
35																	

ASR74-131

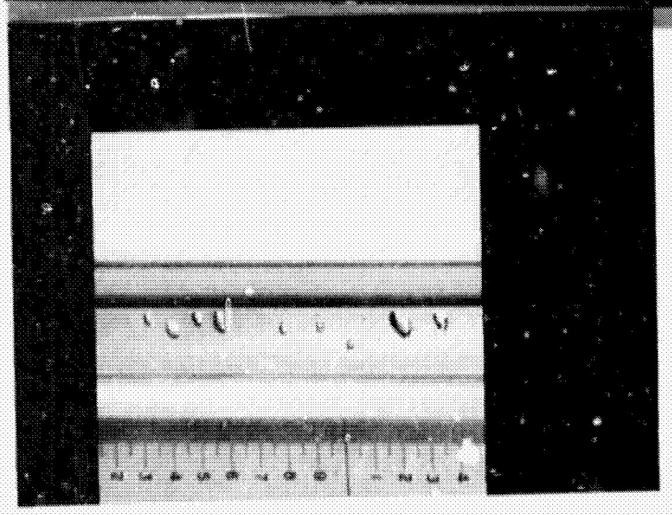

2 Percent (By Volume)

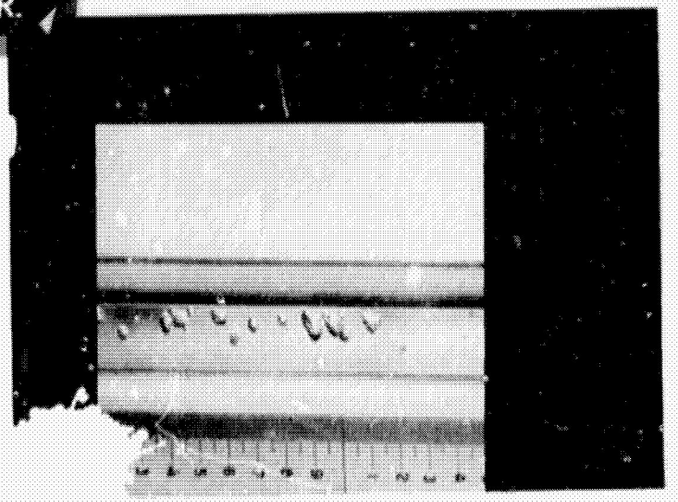

5 Percent (By Volume)

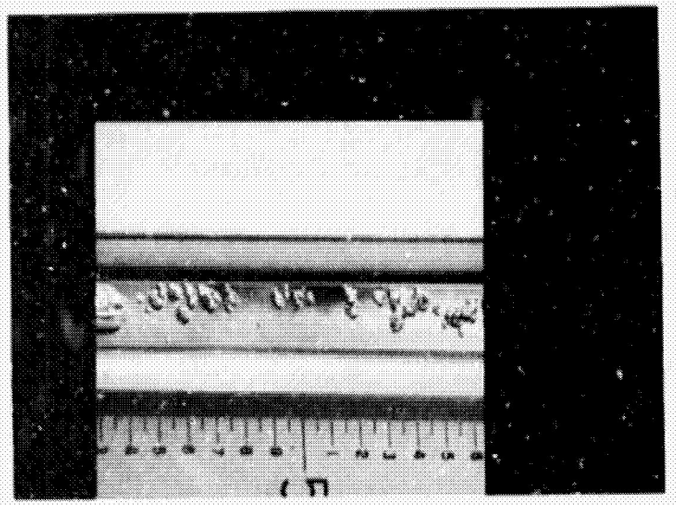

20 Percent (By Volume)

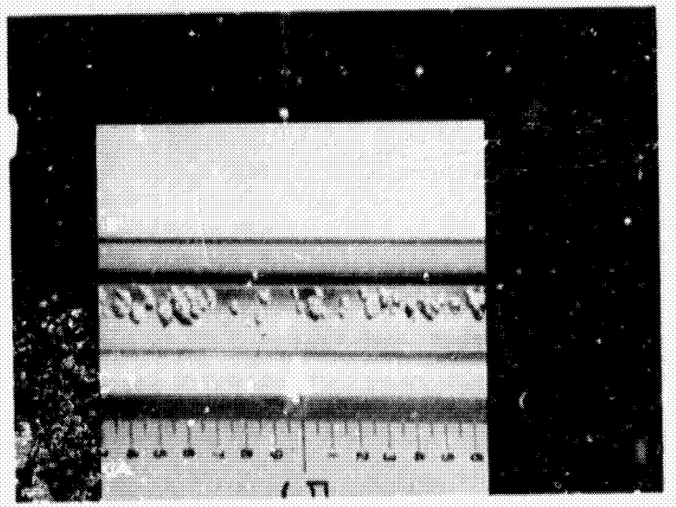

25 Percent (By Volume)

Figure 12. Helium Froth Flows As Viewed Through Downstream Light Tube

coolant velocity (without helium) were, therefore, about 1.5 BTU/in^2-sec and 15 ft/sec, respectively. The subcooling was essentially unchanged since this factor is based only on total flowrate and electrical power.

Actual hot-fire testing of the Integrated Thrust Chamber at NSTF indicated lower than predicted heat loads as discussed in the ITC Test Report. Based on these results, the ITC was reanalyzed to determine probable injector-end heat flux levels and subcooling. This analysis indicated a nominal injector-end heat flux of about 1.5 - 1.6 BTU/in^2-sec. The reduced heat load resulted in an increased outlet subcooling of about 170°F.

The overall result of the various factors discussed previously is that the heated tube test conditions were more severe than currently anticipated for the ITC (based on 1-D heat flux levels). The test heat flux level is comparable, but the experimental value of the velocity times subcooling ($V\Delta T_{SUB}$) factor is about 40 percent of that predicted for the OME Integrated Thrust Chamber.

In spite of the more severe operating conditions, helium froth flows as high as 30 percent by volume were accommodated by the electrically heated tubes without any apparent hardware damage or temperature excursions.

Five tests (4 MMH, 1 50-50) were conducted at increasing heat flux levels in order to determine the burn-out limits associated with helium froth. Only one test was accomplished with the 50-50 coolant (helium froth $\approx$30 percent by volume) as the test section physically "burned-out" after transition to film boiling occurred. Three burn-out type tests (transition to film boiling) were accomplished with MMH at helium flows of 12 and 29 percent by volume. The system power shut-off was sufficiently rapid to prevent actual tube failure during these tests.

The single 50-50/helium froth burn-out point is compared in Figure 13 with the previous heated tube data for 50-50 cooling in terms of burn-out

FIGURE 13

EXPERIMENTAL BURNOUT HEAT FLUX DATA FOR 50-50

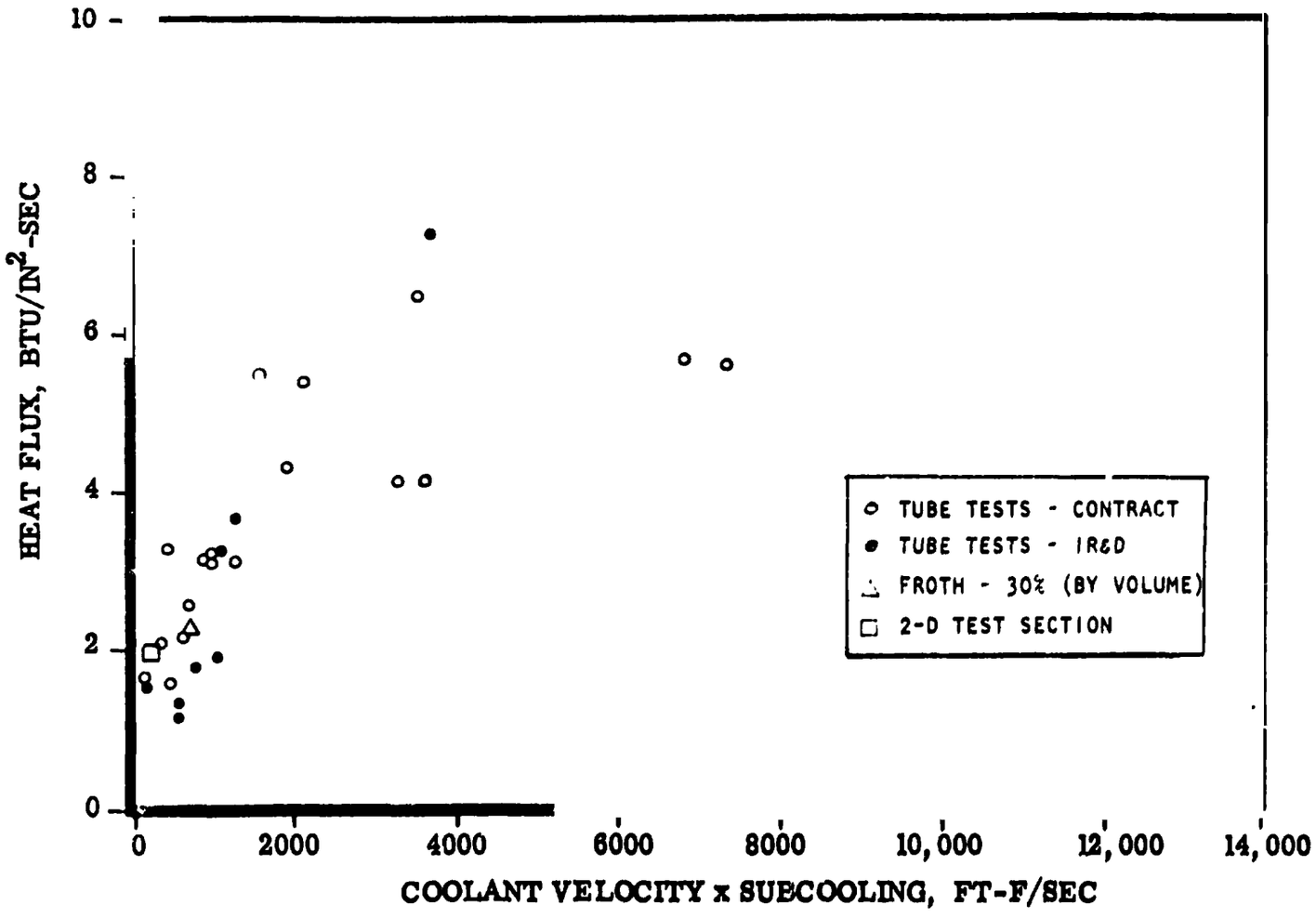

Figure 13

heat flux and the $V \Delta T_{SUB}$ correlating parameter. The froth velocity is based on the reduced density associated with the froth flow.

It appears that the effect of helium ingestion in the form of froth does not significantly affect the 50-50 cooling capability in terms of the basic burn-out relation. A single froth data point, however, is not sufficient to make a firm conclusion particularly considering the scatter of the basic 50-50 burn-out data.

The three MMH/helium froth burn-out data points are compared to the previous heated tube data in Fig. 14. There appears to be a definite degradation in burn-out limits as the helium percent is increased. At a helium flow of 29 percent by volume the burn-out heat flux is about 1.8 BTU/in^2-sec versus about 2.8 BTU/in^2-sec based on previous (no-froth) tests. This represents a significant reduction in the regenerative chamber safety factor if true.

One item which somewhat clouds the MMH/helium froth tests results is the burn-out heat flux level achieved in a relatively low-froth flow ($\simeq$ 4 percent helium) test (#2-67). This test was conducted to approximate the previous no-froth test results. Unfortunately, the burn-out heat flux level obtained was similar to that achieved with 29 percent helium froth. Test 2-67 was conducted at a later date than the helium froth series and there was insufficient time to repeat the test. The test had some inconsistancies such as a negative heat balance (i.e., heat absorbed by coolant greater than electrical power input). The test also utilized a new power source and was conducted somewhat hurriedly (the facility had to be vacated due to other test program commitments). These factors are not necessarily sufficient to invalidate the test, but do suggest the possibility of error.

At present, it must be concluded that there is a strong possibility of a burn-out heat flux reduction with helium froth ingestion. This is

EXPERIMENTAL BURNOUT HEAT FLUX DATA FOR MMH

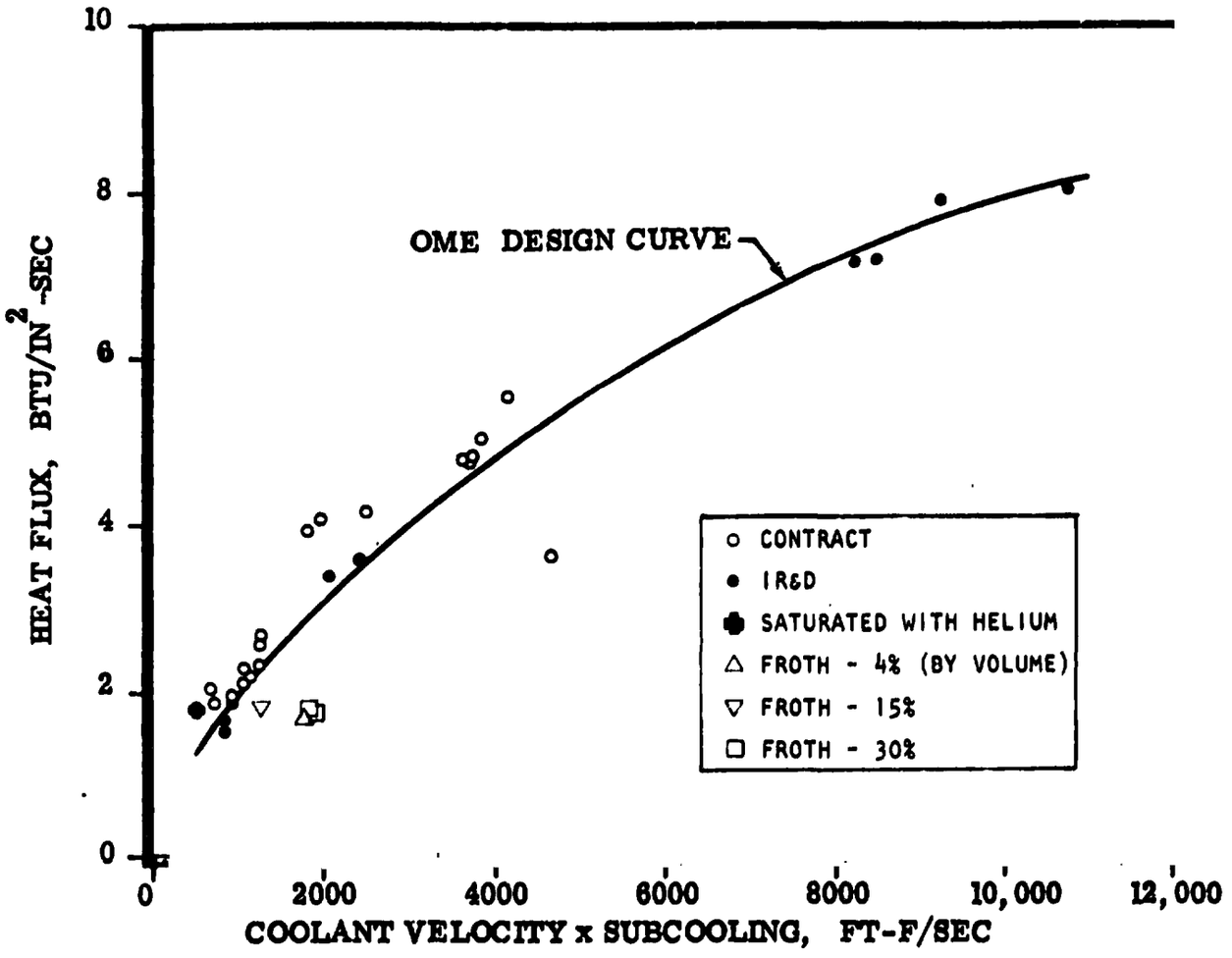

Figure 14

not unreasonable since the presence of numerous small helium bubbles dispersed throughout the liquid may affect the nucleate boiling phenomena. In particular, an MMH bubble formed at the heated surface and dispersed into the main flow may be replaced by helium rather than liquid at the heated surface. Also, the MMH vapor bubble may not condense as rapidly if trapped by helium instead of the subcooled liquid.

Additional testing of helium ingestion in the form of froth is advised to more accurately determine burn-out characteristics. The use of asymmetrically heated rectangular channel test sections should be utilized to simulate actual regenerative cooled thrust chamber operation.

2-D Burn-Out Tests

One of the primary objectives of the additional testing was to determine the 2-D thermal characteristics of a rectangular channel section subjected to asymmetric heating similar to that which occurs in actual thrust chamber operation. Theoretical analysis predicts a concentration of heat in the corners of the channels for the relatively wide lands at the chamber injector end. The predicted reduction of the local injector-end safety factor by about 20 to 30 percent has considerable impact on regenerative chamber design in terms of coolant pressure drop. The asymmetric heated channel tests were conducted to determine the validity of the analysis.

A total of seven burn-out type tests were conducted with amine fuel cooling in two different geometry rectangular channel test sections. These seven tests were evaluated in order to ascertain possible 2-D conduction effects on local safety factor.

The electrical heat generation distribution was estimated using the Differential Equation Analyzer Program (DEAP) thermal model (see Appendix). It was determined from this analysis that about 10 to 15 percent of the

heat generated occurred in the lands and closeout of the test section. The overall asymmetric heat flux (obtained from dividing heat input by copper strip surface area) was therefore adjusted downward by this amount to simulate the actual burnout heat flux condition on the primary heated surface.

In the initial test program, a single burn-out type test was conducted with 50-50 coolant. The test section geometry simulated the demonstrator chamber injector-end design. At nominal flow conditions the electrical power was increased to the maximum facility capability which resulted in a heat flux level of about 2.0 BTU/in^2-sec. As no burn-out occurred, the flowrate was gradually reduced until a wall temperature excursion was achieved. The temperature rise was sufficient to melt the copper heating strip and automatic power shutdown was initiated. This occurred at about one-third of nominal design flow. The various cooling parameters at burn-out are presented in Table 8.

In the later test series, six burn-out type tests were achieved with MMH fuel. A larger power supply was utilized to permit investigation of increased heat flux levels. These results are also presented in Table 8.

The 2-D burn-out results are also presented in Fig. 15 for comparison with the 1-D tube data. It is apparent that at relatively high values of the $V \cdot \Delta T_{SUB}$ parameter the 2-D burn-out heat flux is considerably less than the 1-D value. At lower values of $V \cdot \Delta T_{SUB}$ there is good agreement with 1-D results. The two tests (#2-48 and 2-64) which deviate the most from the tubular 1-D data had the best heat balances (5 and 12 percent). The heat balance on three of the remaining tests was about 25 percent. A detailed re-evaluation of the raw data did not uncover the reason for the discrepancy although it is most likely associated with temperature rise and/or flowrate measurements rather than electrical power measurement. The poor heat balance for Test 2-62 is attributed to inaccuracies in flow measurement due to the extremely small flowrate utilized in this test.

TABLE 8

SUMMARY OF BURN-OUT TESTS IN RECTANGULAR CHANNELS

Coolant	Test No.	Test Section No.	Test Section Length (In)	Coolant Velocity (Ft/Sec)	Coolant Outlet Temp (F)	Coolant Outlet Pressure (psig)	Subcooling $T_{SAT} - T_B$ (F)	$V \Delta T_{SUB}$ (Ft-F/Sec)	*Adjusted Heat Flux (BTU/In^2-Sec)	**Heat Balance (%)
50-50	1-109	1	7.0	7.7	311	171	37	285	2.0	2.3
MMH	2-48	2	7.0	41.8	140	174	227	9490	4.1	5.3
	2-59	3	6.0	11.6	241	148	113	1310	2.5	25.5
	2-60	3	6.0	20.9	215	154	141	2950	3.7	27.2
	2-62	1	4.5	1.6	280	168	85	134	1.0	48.0
	2-63	1	4.5	7.5	207	159	151	1130	2.3	23.9
	2-64	1	4.5	21.2	156	149	199	4220	3.7	12.3

*Adjusted for heat generation in steel lands and closeout

**Heat balance = $1 - (Q_{out}/Q_{in})$

EXPERIMENTAL BURNOUT HEAT FLUX DATA FOR MMH

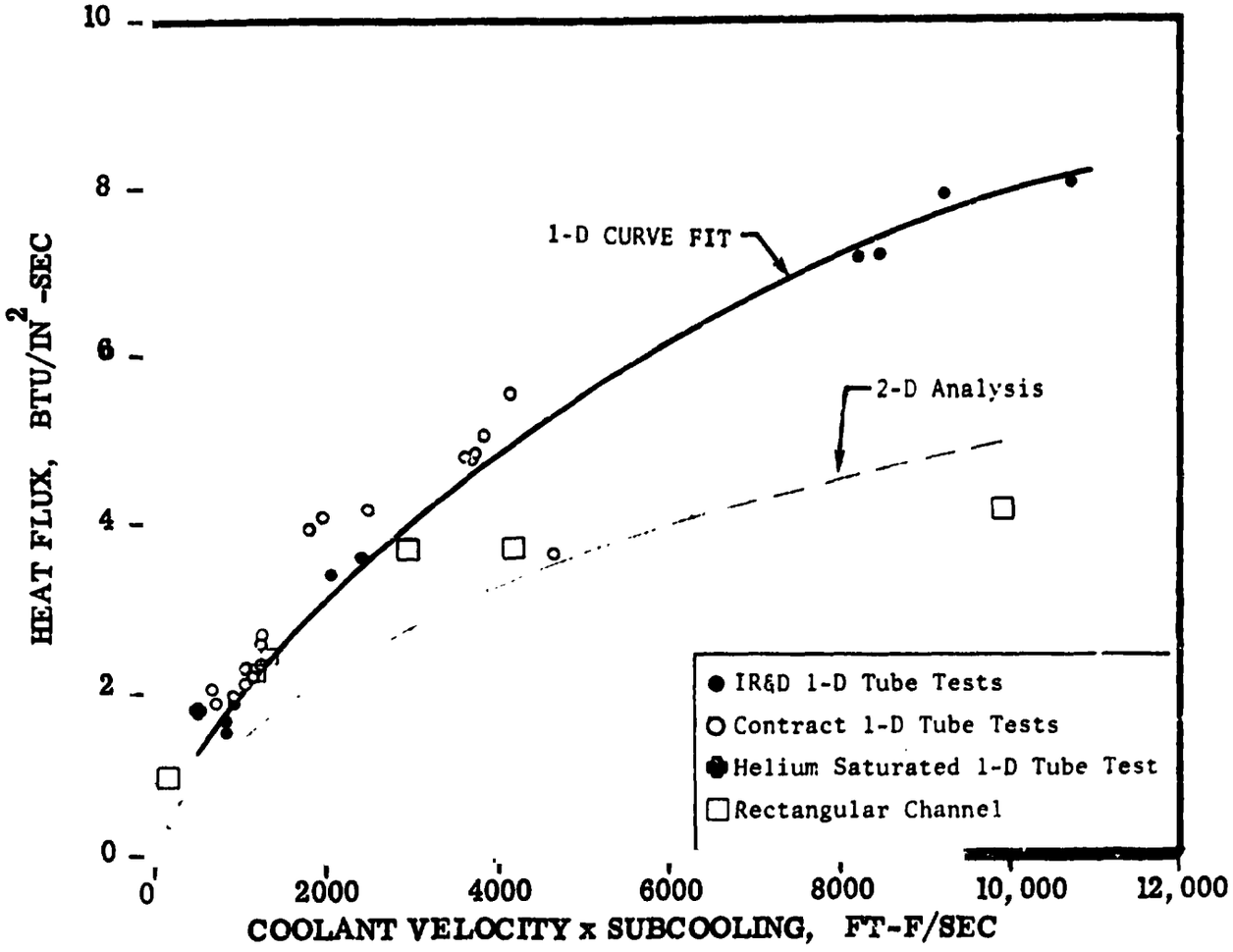

Figure 15

An analytical prediction of the burn-out heat flux as a function of the $V\Delta T_{SUB}$ parameter was determined using the aforementioned DEAP thermal model and channel geometry of test sections number 1 and 2 (H = .080", W = .060", L = .090"). The resulting analytical curve is also presented in Fig. 15 where it is seen to agree reasonably well with the rectangular channel test results.

At the low heat flux where the data appears to agree better with the 1-D results rather than the 2-D analysis, it is possible that some localized film boiling was sustained. This could be possible if the film boiling characteristics of MMH are better than assumed.

Based on the foregoing analysis, it can be concluded that the use of a one-dimensional safety factor (as obtained with symmetrically heated tubes) can lead to overestimation of the safety factor associated with rectangular channels. The DEAP thermal model (2 dimensional analysis) appears to provide a reasonably accurate means of estimating local safety factors associated with rectangular channels. A 2-dimensional analysis approach was used in designing both the Demonstrator and Integrated thrust chambers on this program.

CONCLUSIONS

The results obtained during this test program provided valuable information regarding cooling characteristics of MMH and 50-50 fuel under various adverse operating conditions, as might occur in the OME regenerative chamber.

Both MMH and 50-50 are capable of withstanding chamber hot-start conditions at initial wall temperatures as high as 1600 F without adverse effects on either chamber or coolant. The initial rapid quench occurs without wall temperature overshoot or fuel "popping."

Helium bubble ingestion durations in excess of one second are feasible in the OME thrust chamber without serious wall temperature increase. The asymmetric heated rectangular test sections simulating the OME chamber exhibited much less sensitivity to helium bubbles than did the uniformly heated circular tube test sections.

Helium froth ingestion tests in circular tubes indicated steady-state operating capability with froth percents as high as 29 percent (by volume) at conditions more severe than predicted for the OME. The maximum burn-out heat flux capability of MMH appeared to be degraded significantly, however, at these higher helium froth flows. Further testing is advised. In particular, the use of an asymmetrically heated rectangular test section is recommended to verify safe operation with froth at simulated OME chamber conditions.

The 2-D test results essentially verified the predicted safety factor penalty associated with wide lands such as occur in the OME constant channel width chamber designs at the injector end. This effect can be eliminated by utilizing a tapered channel width OME chamber design, which will provide for narrower lands at the injector end. This approach should result in significant coolant pressure drop reduction as compared to the current designs for an equivalent true local safety factor profile.

APPENDIX

THERMAL ANALYSIS OF ELECTRICALLY HEATED RECTANGULAR PASSAGE TEST SECTIONS COOLED WITH AMINE FUELS

Rocketdyne recently completed a series of tests under contract NAS9-12802 to determine cooling characteristics of MMH and 50-50 fuel. These tests utilized rectangular coolant passage test sections electrically heated along one surface to more closely simulate the coolant channel heat and temperature distribution that occur in an actual thrust chamber. The analytical technique used in evaluating the test results obtained with the asymmetrically heated, rectangular coolant passage test sections is presented in this appendix.

DISCUSSION

The primary purpose of the electrically heated test section tests (tube and rectangular passages) conducted to date with amine fuels is to establish a semi-empirical correlation and/or thermal model to predict the conditions under which transition to film boiling will occur in a regenerative cooled thrust chamber such as the SS/OME. This transition to film boiling from the nominal forced convection-nucleate boiling cooling mode is commonly referred to as a burn-out condition, since the increased thermal resistance of the film to the imposed heat flux level usually results in excessive wall temperatures and localized structural failure.

The heat flux at which burn-out occurs is primarily a function of the coolant velocity, V, and sub-cooling, ΔT_{SUB} (saturation temperature minus local coolant temperature). A typical plot of electrically heated circular tube data for MMH cooling is presented in Fig. A1. A satisfactory correlating equation based on this data is also shown and can be expressed as

$$(Q/A)_{B.O.} = 0.025\ (V \cdot \Delta T_{SUB})^{0.633} \qquad \text{(A-1)}$$

FIGURE A1

EXPERIMENTAL BURNOUT HEAT FLUX DATA FOR MMH

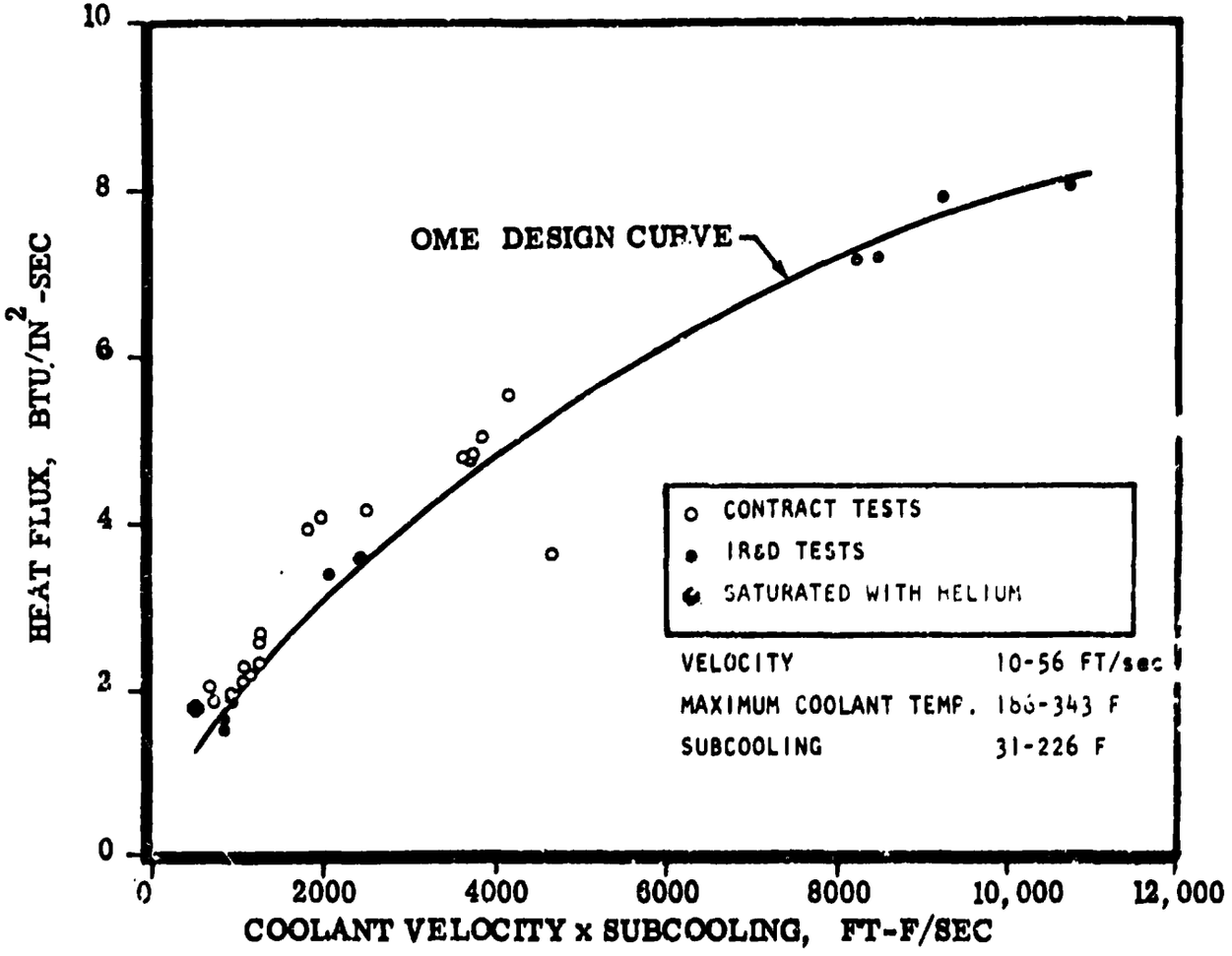

where V is in ft/sec, ΔT_{sub} in ^{o}F, and $(Q/A)_{B.O.}$ in BTU/in^{2}-sec. This equation is somewhat conservative in that it predicts zero heat flux capability if either the velocity or subcooling is zero.

The aforementioned data is based on a uniformly electrically heated circular tube and, as such, can be considered basic cooling data. In order to apply these results to noncircular and/or asymmetric heated test sections, it is necessary to utilize an appropriate two-dimensional conduction model to obtain the effective heat flux distribution at the coolant surface interface. This effective 2-D heat flux in conjunction with the essentially 1-D equation (A-1) determines the relative local safety factor defined as:

$$S.F. = \frac{(Q/A)_{B.O.}}{(Q/A)_{local}} \qquad (A-2)$$

In the case of the OME thrust chamber, the cooling passages are rectangular with the combustion gas convective heat input occurring over one surface. This is shown pictorially in Fig. A2. In order to simulate the thrust chamber asymmetric heating on a single channel subscale test, a copper strip is brazed to one surface of the basic CRES channel test section. This is also depicted in Fig. A2. The large difference in electrical resistivity of copper and CRES results in the majority of heat generation in the copper ($\simeq$80-90 percent), thereby simulating thrust chamber asymmetric heating.

The 2-D conduction analysis was accomplished using the Rocketdyne Differential Equation Analyzer Program (DEAP). This is a thermal analyzer type program, which utilizes a lumped parameter nodal network consisting of the appropriate node capacitance and inter-node connectors

PREPARED BY	ROCKETDYNE A DIVISION OF NORTH AMERICAN ROCKWELL CORPORATION	PAGE NO OF
CHECKED BY		REPORT NO
DATE		MODEL NO

FIGURE A2

(admittance) to represent the desired geometry. A schematic nodal representation of the electrically heated rectangular channel geometry is presented in Fig. A5. Note that only a half-channel section is required due to symmetry. In the case of the thrust chamber analysis, the copper section is replaced by CRES (total thickness equalling the hot wall value), resulting in a finer grid (six divisions) across the hot wall.

The electrical heating is simulated by internal heat generation functions for each node. In the case of a 2-D model, the electrical heat generation per unit length Q/ℓ can be expressed in terms of impressed voltage per unit length E/ℓ as:

$$Q/\ell = \left(\frac{E}{\ell}\right)^2 \frac{A_n}{r} \qquad \text{(A-3)}$$

where A_n represents the cross-sectional area assigned to each node, and r is the electrical resistivity corresponding to the node material. The total heat generation can be varied by simply inputting into the program various values of E/ℓ.

The electrical resistivity of copper is strongly affected by temperature as can be seen in Fig. A4, where the resistivity increases about a factor of 4 in going from room temperature to 1200 F. This effect is accounted for in the DEAP program by means of an input table such that the resistance of each node is based on its calculated temperature. The variation in CRES resistivity with temperature is much less than for copper varying only about a factor of 1.5 for the same temperature range noted previously. This is depicted in Fig. A5.

The conduction and heat generation portion of the channel thermal model just discussed is relatively simple and straightforward. The primary difficulty in the thermal analysis is the specification of the coolant

PREPARED BY	ROCKETDYNE A DIVISION OF NORTH AMERICAN ROCKWELL CORPORATION	PAGE 0 OF
CHECKED BY		REPORT NO
DATE		MODEL NO

FIGURE A3

A.[illegible] SCHEMATIC [illegible] ELECTRICALLY HEATED [illegible] SECTION

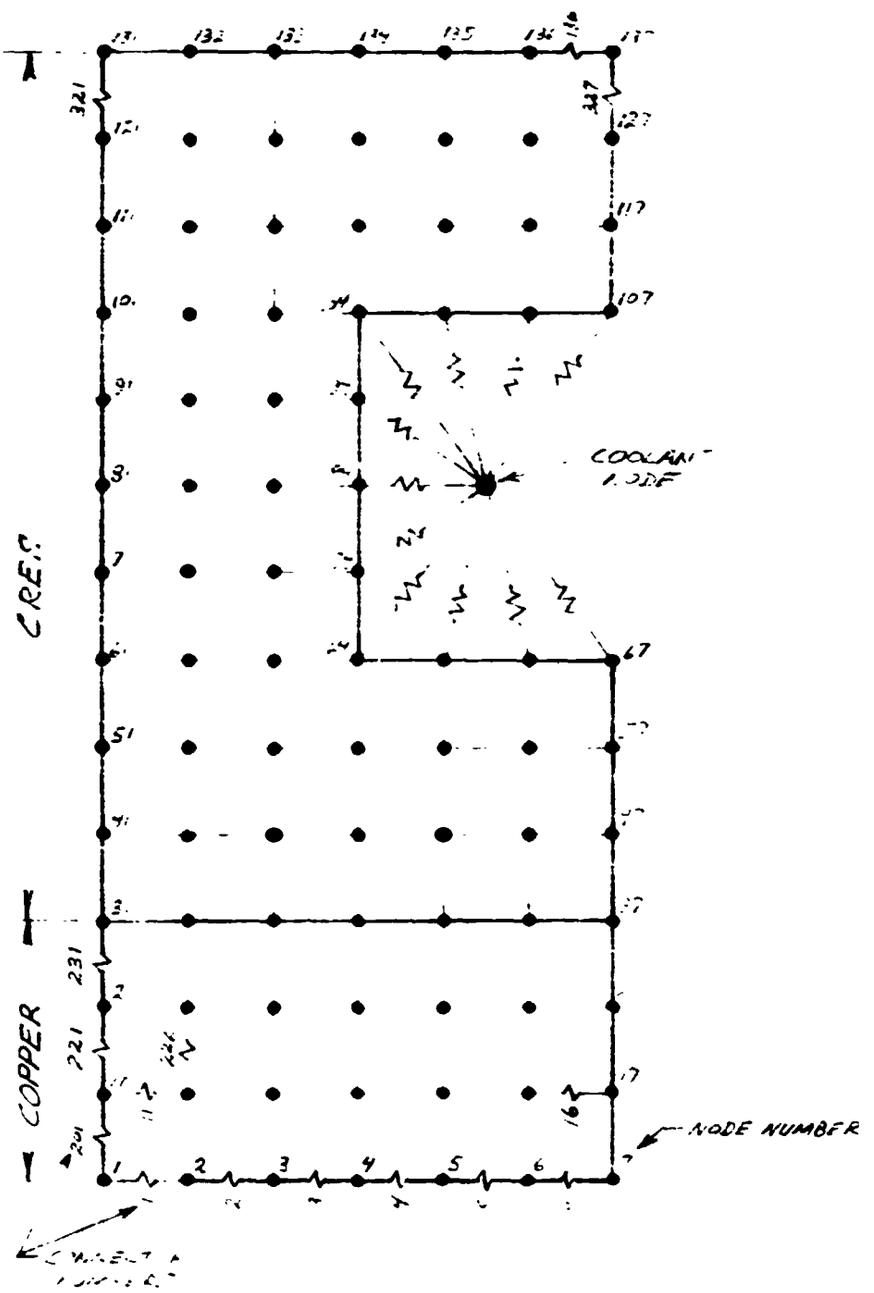

FIGURE A4
ELECTRIC RESISTIVITY OF COPPER
AS A FUNCTION OF TEMPERATURE

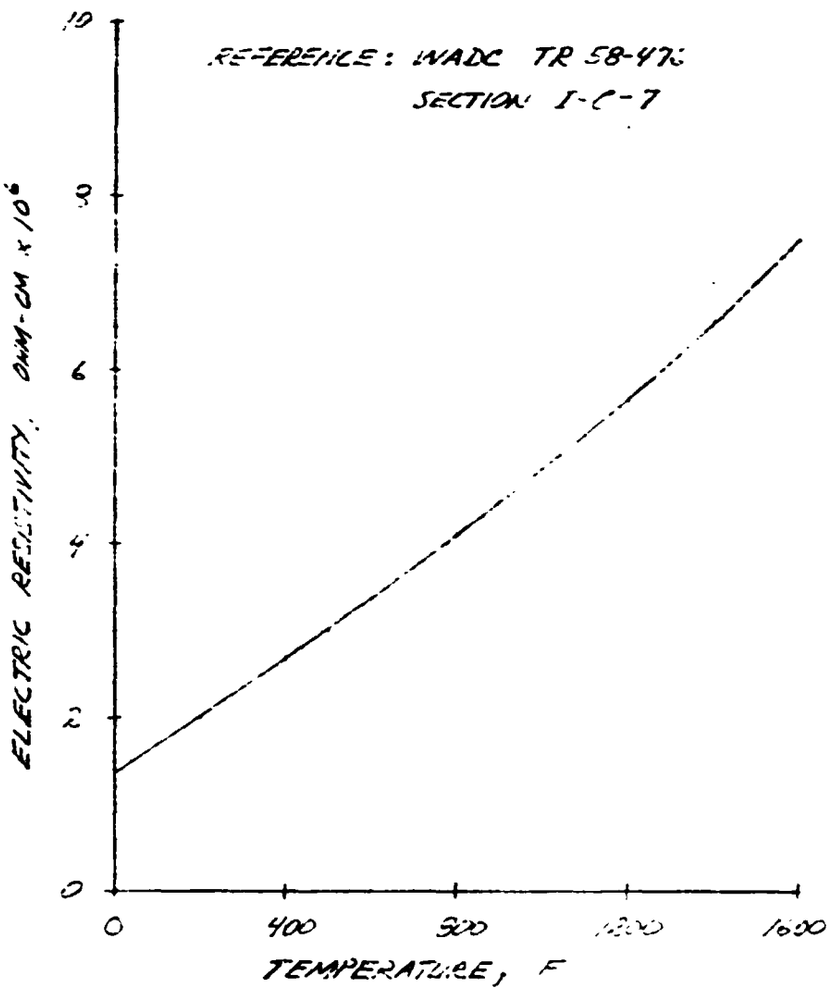

EDT 4/15/74

FIGURE A5

ELECTRIC RESISTIVITY OF CRES AS A FUNCTION OF TEMPERATURE

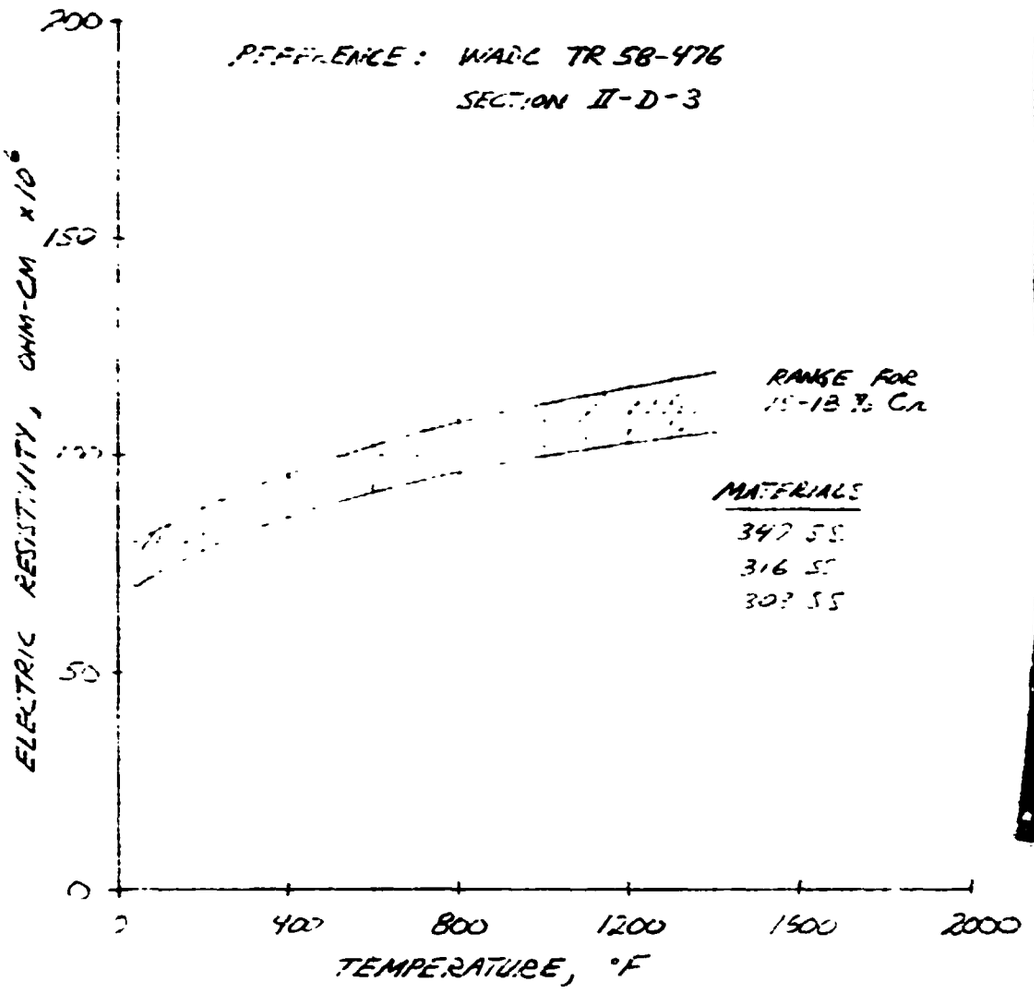

P.D.T. 4/15/...

side boundary conditions associated with the forced convection-nucleate boiling mode of cooling encountered in the OME thrust chamber design.

In simple forced convection the thermal resistance is essentially independent of the imposed heat transfer rate. The thermal resistance associated with nucleate boiling, however, decreases markedly with increasing heat transfer rate due to an increased rate of vapor bubble formation and agitation, until a point is reached wherein the bubble generation rate is so great that a vapor film is formed between the wall and liquid. This point is known as transition to film boiling, and is characterized by very high thermal resistance with possible resultant tube or channel burn-out due to the high temperature drop across the film.

In the DEAP program, the wall coolant surface boundary conditions are specified in terms of a local bulk temperature, T_B, and a film coefficient h_c such that the heat flux of a surface node at a temperature, T_{wc}, is given by the usual relation:

$$Q/A = h_c (T_{wc} - T_B) \qquad (A-4)$$

Since the film coefficient is inversely proportional to the coolant thermal resistance, it varies just the opposite of the cooling mode-heat flux relation discussed in the previous paragraph. That is, for forced convection, h_c is relatively constant, increases markedly in the nucleate boiling regime and finally drops to a very low value during film boiling.

Based on the preceding discussion, it is apparent that a film coefficient-heat flux relationship must be established that is compatible for use in the thermal model. This is most easily accomplished by consideration of the wall temperature variation with cooling mode. Local nucleate boiling cannot be initiated until the local wall temperature exceeds the coolant saturation temperature, T_{SAT}. Transition to film boiling

occurs about 50 to 100 F above saturation temperature (critical ΔT). Using these temperature bounds for nucleate boiling, the effective film coefficient can be expressed as a function of wall temperature as shown schematically in Fig. A6.

For coolant side wall temperatures below T_{SAT}, the film coefficient is that calculated for forced convection from the standard relationship:

$$h_c = 0.023 \frac{k}{d_H} N_{RE}^{0.8} N_{PR}^{0.4} \qquad \text{(A-5)}$$

where d_H is the passage hydraulic diameter, k the coolant thermal conductivity and N_{RE} and N_{PR} are coolant Reynolds and Prandtl number, respectively.

At a coolant side wall temperature equal to T_{SAT} + 100 F (this represents about the maximum temperature differential possible before film boiling occurs), the effective film coefficient is determined from the 1-D burn-out heat flux in conjunction with the corresponding wall to coolant temperature difference:

$$h_c = \frac{(Q/A)_{B.O.}}{(T_{SAT} + 100) - T_B} \qquad \text{(A-6)}$$

where $(Q/A)_{B.O.}$ is obtained from equation (A-1) or other suitable relation based on electrically heated tube data. The linear $h_c - T_{wc}$ relation utilized between maximum and minimum boiling points is sufficiently accurate since the maximum ΔT_w is 100 F.

In the film boiling region, the film coefficient is estimated at about 10 percent of the peak value based on limited water film boiling data. The actual value is not particularly important, since the purpose of the current analysis is to determine the point at which film boiling is

PREPARED BY	ROCKETDYNE A DIVISION OF NORTH AMERICAN ROCKWELL CORPORATION	PAGE NO OF
CHECKED BY		REPORT NO
DATE		MODEL NO

FIGURE A6

SCHEMATIC REPRESENTATION OF EFFECTIVE FILM COEFFICIENT AS A FUNCTION OF COOLANT SIDE WALL TEMPERATURE

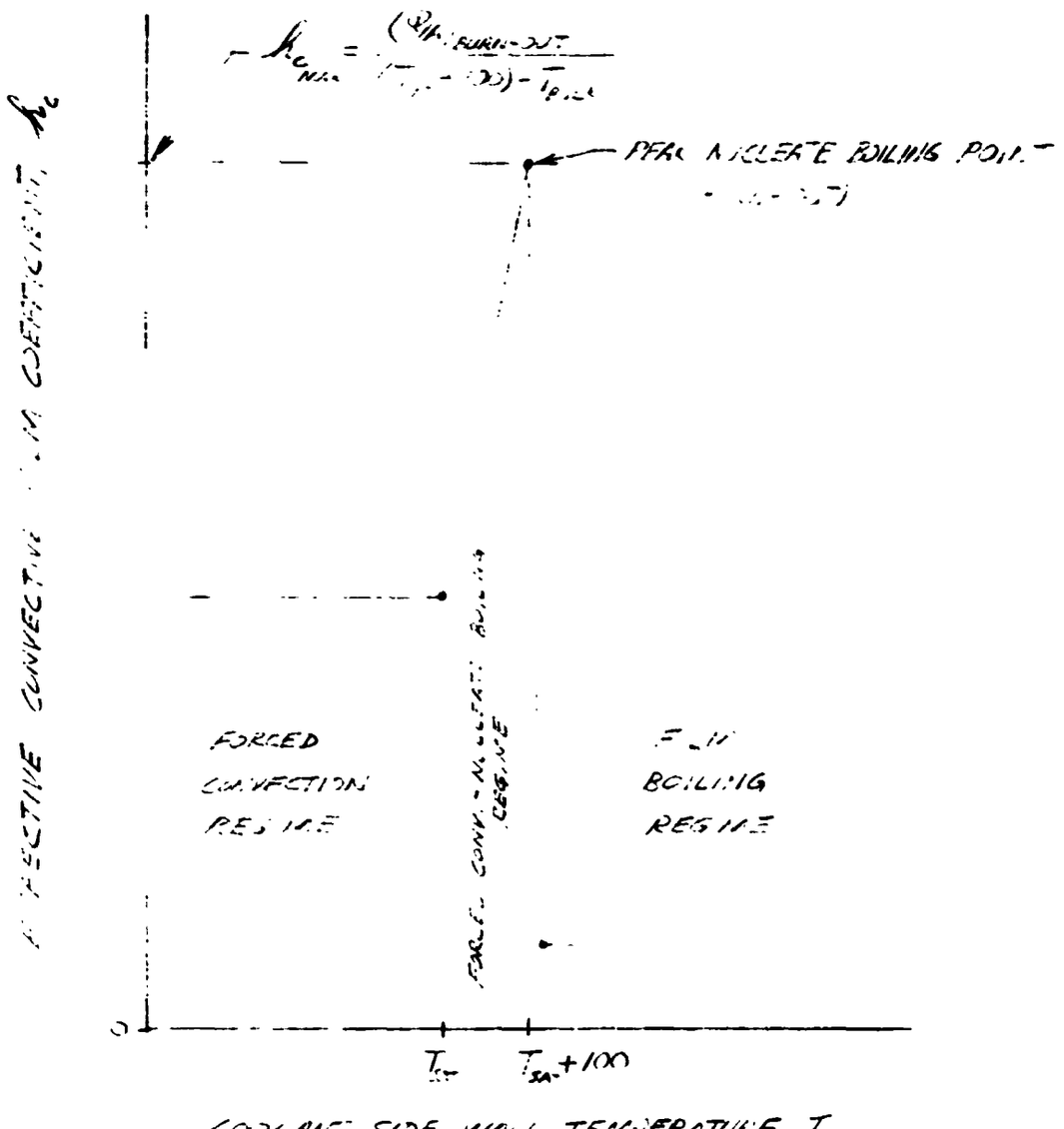

initiated in a channel section. Accurate estimation of the film boiling effective film coefficient would be of great value, however, in determining the equilibrium temperature of the channel wall and whether a "burn-out" would actually occur. This type of basic da a is difficult to obtain and would require somewhat more elaborate test procedures than utilized in previous electrically heated tube tests.

The preceding film coefficient-coolant wall temperature relation was incorporated into the DEAP model to provide more accurate determination of the wall temperature and heat flux distribution around to channel coolant surface.

The DEAP thermal model was utilized to determine the electrical power requirements to initiate film boiling corresponding to the coolant velocity, bulk temperature and saturation temperature for actual test conditions. The program input heat load (power) was gradually increased until a wall temperature excursion simulating burn-out was predicted. Typical results are shown in Fig. A7 and A8 for coolant conditions corresponding to Test 48 as noted. In Fig. A7 transition to film boiling does not occur, and the various wall temperatures achieve an equilibrium value. In Fig. A8, a nominal heat load increase of about 7 percent, compared to the previous case, results in initiation of film boiling in the corner (node 64) and moving outward to mid-channel (node 67).

The temperature and heat flux distribution corresponding to a heat load condition slightly below a burn-out value is presented in Fig. A9. The relative shape and spacing of the isotherms indicates a concentration of heat in the channel corner. The calculated heat flux distribution is shown to be a maximum in the corner with a vlaue of about 7.8 BTU/in^2-sec. The burn-out heat flux based on equation (A-1) for the coolant conditions noted is 7.9 BTU/in^2-sec. The average surface heat flux in the copper strip and top CRES section is 5.0 BTU/in^2-sec obtained by dividing the heat generated by the thermal model test section half width. This

FIGURE A7

TEMPERATURE RESPONSE WITHOUT TRANSITION TO FILM BOILING

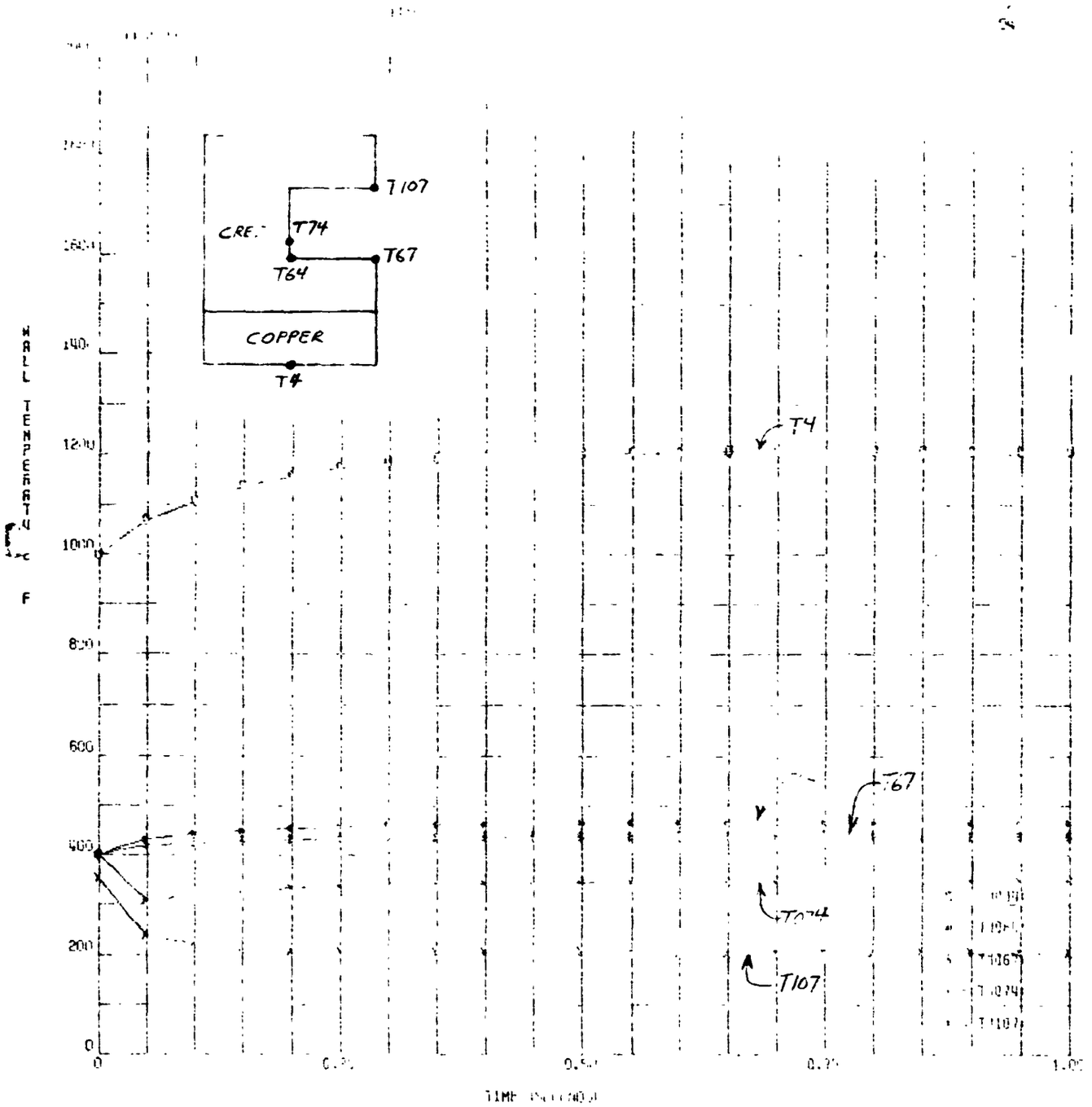

FIGURE A.P.

TEMPERATURE RESPONSE WITH TRANSITION TO FILM BOILING

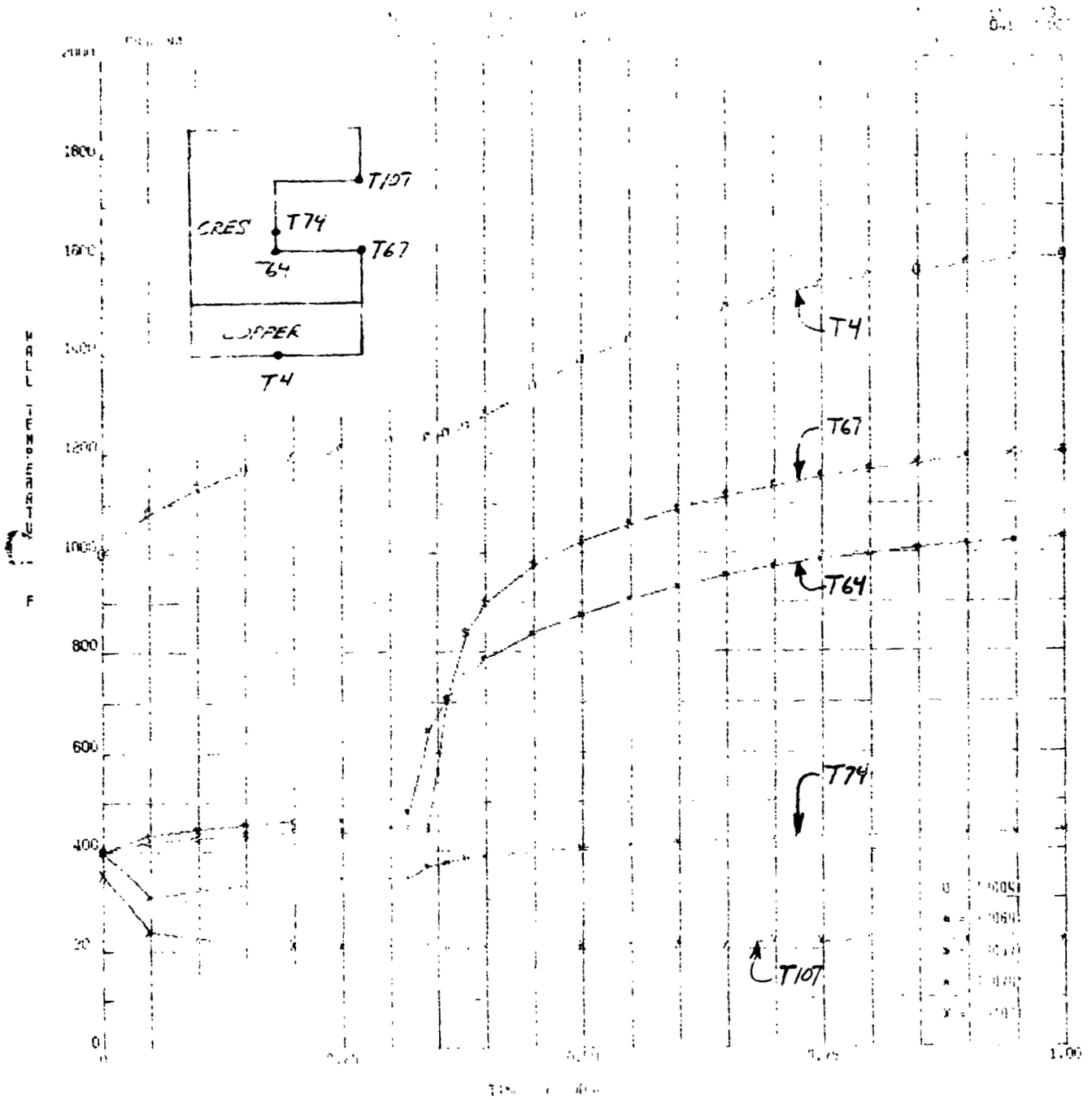

FIGURE A9

ISOTHERMS FOR ELECTRICALLY HEATED CHANNEL

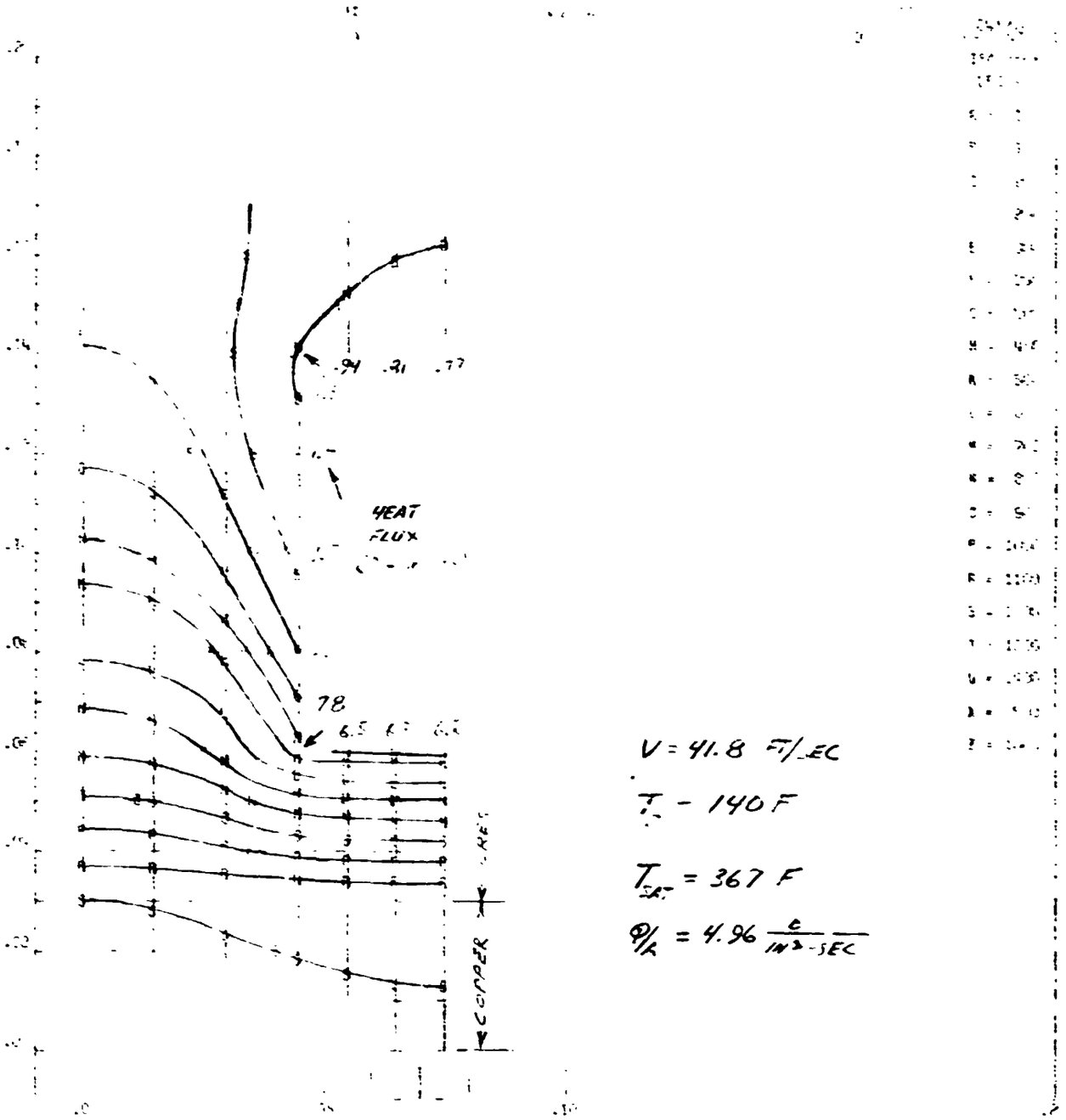

latter value is the equivalent 1-D heat flux which would normally be used to predict the local safety factor neglecting coolant passage geometry effects. It is apparent that the relatively wide lands in this channel design result in considerable penalty insofar as actual coolant safety factor is concerned.

The actual 1-D equivalent coolant burn-out heat flux as determined experimentally for test 48 was about 4.1 BTU/in^2-sec after subtracting out the heat generated in the lands and closeout ($\simeq$13 percent).

One further consideration is whether or not the asymmetric electrically heated rectangular test section is an accurate representation of actual thrust chamber operating conditions. It would be expected, for example, that the high thermal conductivity copper strip would tend to smooth out the heated surface temperature distribution. In addition, the electrical heat generation in the CRES lands and closeout represent an increase in total heat load to the test section not found in actual thrust chamber operation.

The DEAP thermal model was, therefore, utilized to determine the heat flux and temperature distribution in the test section (minus the copper strip) subjected to a convective heat input rather than an electrical equivalent. The resulting isotherms and heat flux levels are presented in Fig. A10. There is, indeed, a difference in the heated surface temperature distribution with a variation of about 180 F from mid-channel to mid-land, rather than 13 F as in the electrically heated channel analysis. The average surface temperature, however, is similar in each case being about 1200 F. The closeout region is about 65 F cooler without the electrical heat input. The key factor, however, is the corner heat flux which is seen to be only about 6 percent lower than for the electrical heating case. It appears, therefore, that an asymmetric electrically heated rectangular passage test section is a reasonably accurate representation of actual thrust chamber heating in terms of determining initiation of burn-out conditions.

FIGURE A10

ISOTHERMS FOR CONVECTIVELY HEATED CHANNEL

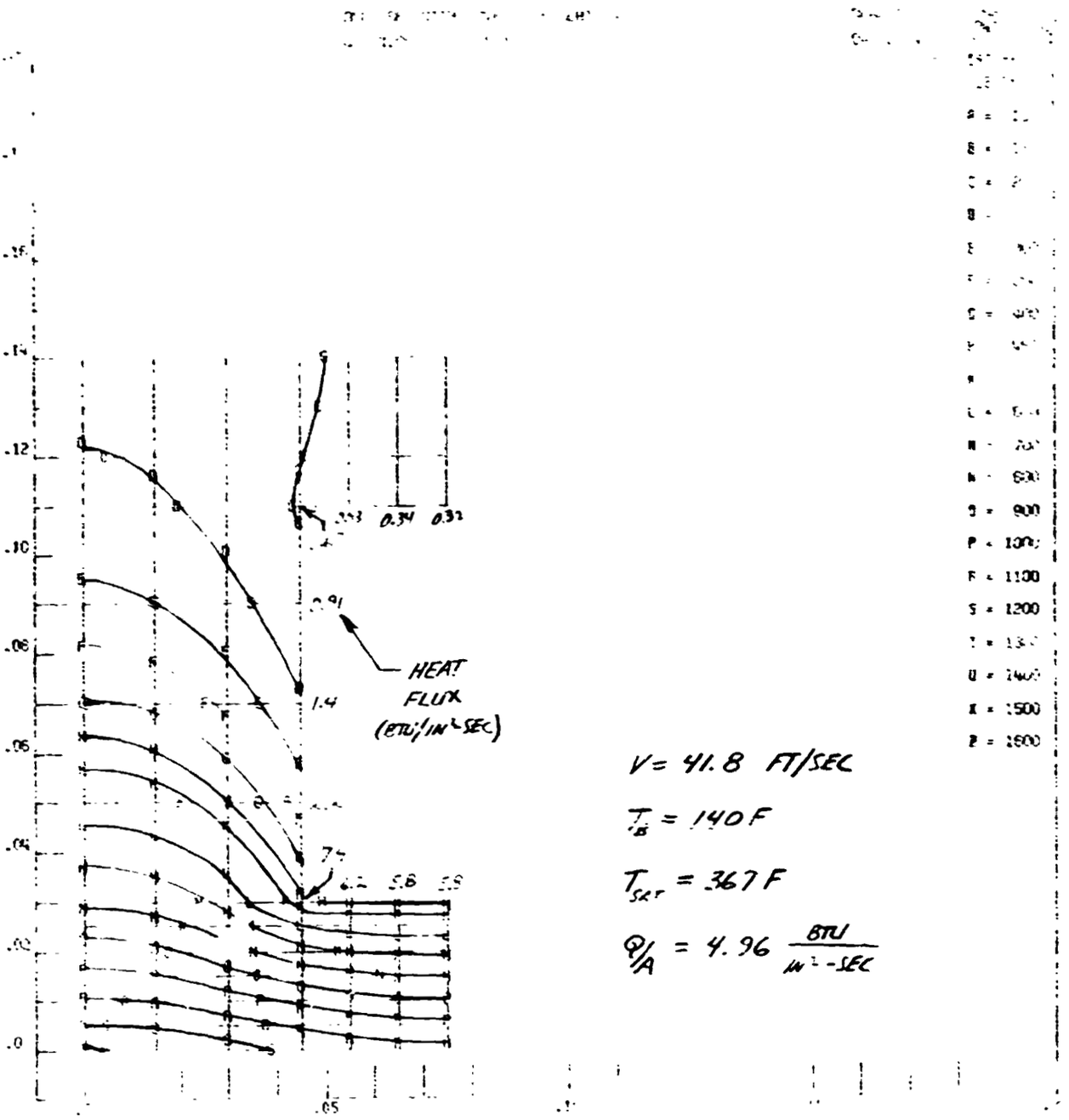

$V = 41.8$ FT/SEC

$T_{IB} = 140$ F

$T_{SAT} = 367$ F

$Q/A = 4.96 \frac{BTU}{IN^2\text{-SEC}}$